Expression and implication of clusterin in left ventricular remodeling after myocardial infarction

Annie Turkieh, Marie Fertin, Marion Bouvet, Paul Mulder, Hervé Drobecq, Gilles Lemesle, Nicolas Lamblin, Pascal de Groote, Sina Porouchani, Maggy Chwastyniak, et al.

Expression and implication of clusterin in left ventricular remodeling after myocardial infarction

Annie Turkieh, PhD[a], Marie Fertin, MD, PhD[a], Marion Bouvet, PhD[a], Paul Mulder, PhD[b], Hervé Drobecq, MSC[c], Gilles Lemesle, MD, PhD[a,d,e,f], Nicolas Lamblin, MD, PhD[a,d,e,f], Pascal de Groote, MD, PhD[a,d], Sina Porouchani, MSC[a], Maggy Chwastyniak, MSC[a], Olivia Beseme, MSC[a], Philippe Amouyel, MD, PhD[a,e,g], Frédéric Mouquet, MD, PhD[d], Jean-Luc Balligand, MD, PhD[h], Vincent Richard, PhD[b], Christophe Bauters, MD[a,d,e,f], Florence Pinet, PhD[a]

[a]INSERM, Univ. Lille, CHU Lille, Institut Pasteur de Lille, FHU-REMOD-VHF, U1167 - RID-AGE - Facteurs de risque et déterminants moléculaires des maladies liées au vieillissement, F-59000 Lille, France

[b]Normandie Univ, UNIROUEN, Inserm U1096, FHU-REMOD-VHF, 76000 Rouen, France

[c]Univ. Lille, CNRS, Institut Pasteur de Lille, UMR 8161 - M3T - Mechanisms of Tumorigenesis and Target Therapies, F-59000 Lille, France

[d]USIC et Centre Hémodynamique, Institut Cœur Poumon, Centre Hospitalier Régional et Universitaire de Lille, F-59000, Lille, France

[e]Faculté de Médecine de l'Université de Lille, F-59000, Lille, France

[f]FACT, French Alliance for Cardiovascular Trials, F-75000, Paris, France

[g]CHU Lille, Service de Santé Publique, Épidémiologie, Économie de la Santé et Prévention, F-59000, Lille, France

[h]Institut de Recherche Experimentale et Clinique, Pole of Pharmacology and Therapeutics and Cliniques Universitaires Saint-Luc, Université catholique de Louvain, Brussels, Belgium.

Corresponding author:

Dr Florence PINET, INSERM U1167-IPL, 1 rue du professeur Calmette, 59019 Lille cedex, France

Tel: (33) 3 20 87 72 15

Fax: (33) 3 20 87 78 94

E-mail: florence.pinet@pasteur-lille.fr

Word count: 4351

ABSTRACT

Background: Left ventricular remodeling (LVR) following myocardial infarction (MI) is associated with an increased risk of heart failure (HF) and death. In spite of a modern therapeutic approach, LVR remains relatively frequent and difficult to predict in clinical practice. Our aim was to identify new biomarkers of LVR and understand their involvement in its development.

Methods and Results: Proteomic analysis of plasma from the REVE-2 study – a study dedicated to the analysis of LVR which included 246 patients after a first anterior MI - identified increased plasma levels of clusterin in patients with high LVR. We used a rat model of MI to analyze clusterin expression in the LV and found a significant increase that was correlated with LVR parameters. We found increased clusterin expression and secretion in primary cultures of rat neonate cardiomyocytes (NCM) hypertrophied by isoproterenol. Silencing of clusterin in hypertrophied NCM induced a significant decrease in cell size, ANP, and BNP expression, associated with a decreased ERK1/2 activity, suggesting a pro-hypertrophic role of clusterin. We then confirmed a significant increase of both intracellular precursor and mature form of clusterin in failing human hearts. Finally, the circulating levels of clusterin (secreted form) were increased in patients with chronic HF who died from cardiovascular cause during a 3-year follow-up (n=99) compared to survivors (n=99).

Conclusions: Our results show for the first time that plasma clusterin levels are associated with LVR post-MI, have a part of cardiac origin and are predictor of early death in HF patients.

INTRODUCTION

Chronic heart failure (HF) remains a major public health problem[1] with a high rate of mortality in spite of recent therapeutic improvements[2]. The most common cause of HF is coronary artery disease and particularly myocardial infarction (MI)[3].

Left ventricular remodeling (LVR) following myocardial infarction is a dynamic and complex process that occurs in response to myocardial damage and is associated with an increased risk of HF and cardiovascular death[4,5]. Post-MI LVR can be divided in two phases. The early phase (occurring few hours to several weeks after MI onset) involves the expansion of the infarct zone, including dilatation and thinning of the infarct zone[6]. The late phase (months, years) involves globally the LV and is associated with time-dependent dilatation, distortion of ventricular shape, mural hypertrophy, as well as structural tissue changes[7]. Although LVR may be considered as a protective mechanism to maintain systolic flow and cardiac “pump” function, this phenomenon leads to alterations of global LV function and ultimately aggravates HF. In two independent prospective echocardiographic studies (REmodelage VEntriculaire, REVE and REVE-2), we observed a 30-40% LVR rate after a first acute anterior wall MI despite high acute reperfusion rates and widespread prescription of secondary prevention medications[8,9]. However, LVR remains difficult to predict in clinical practice and its severity cannot be fully predicted based on its known determinants such as those related to infarct size, anterior infarct location or LV ejection fraction[10]. Circulating biological markers called "biomarkers" may facilitate the diagnosis and the prognosis of LVR and HF[11]. The only biomarker clinically used in MI patients is B-type natriuretic peptide (BNP) whose concentration helps to predict the risk of HF[12], but data on its ability to predict LVR are discordant[9,13,14,15].

Clusterin (CLU) is constitutively expressed in most mammalian tissues and is highly conserved across species. Several functions have been proposed for CLU such as complement activity regulation, lipid transport, apoptosis regulation and cell interaction[16]. Several studies show increased CLU levels in plasma[17,18] and LV[18,19] of MI patients at early stage after MI. Until now, the relationship of plasma CLU levels with LVR post-MI has not been studied despite a recent study showing that CLU is independently associated with chronic HF[20].

In this study, we show for the first time that 1) CLU is increased in late stage after MI and is associated with LVR; 2) CLU expression and secretion are increased by hypertrophied cardiomyocytes and seems play a pro-hypertrophic role and; 3) plasma levels of CLU are predictor of early death in HF patients.

MATERIALS AND METHODS

Detailed information is supplied as supplemental. The data, analytic methods, and study materials will be been made available to other researchers for purposes of reproducing the results or replicating the procedure.

Patients

The studies were approved by the Ethics Committee of the "Centre Hospitalier et Universitaire de Lille" and comply with the Declaration of Helsinski. All patients gave written informed consent.

REVE-2 study

The design of the REVE-2 study has been published in detail elsewhere[9]. We enrolled 246 patients with a first anterior wall Q-wave MI between February 2006 and September 2008. The protocol required serial echographic studies at baseline (day 3 to day 7) and 3 and 12 months after MI. Left ventricular remodeling (LVR) was defined as percent change in EDV from baseline to 1 year. Serial blood samples were taken at discharge (day 3 to day 7), and 1, 3, and 12 months after MI.

INCA study

All patients referred for evaluation of systolic HF (LVEF <45%) in our institution between November 1998 and May 2010 were included in a prospective cohort on prognostic indicators[21,22,23]. From this population, we selected 198 patients included between November 1998 and December 2005, as previously described[24]. Blood sample was obtained at inclusion.

Human heart biopsies

Tissues from failing and non-failing human hearts were obtained respectively from Lille University Hospital (France) and from Catholic University of Leuven (Belgium).

Animal models

All animal experiments were performed according to the Guide for the Care and Use of Laboratory Animals published by the US National Institutes of Health (NIH publication NO1-OD-4-2-139, revised in 2011). MI was induced in 10-week-old male Wistar rats (Janvier, Le Genest St isle, France) by ligation of the left anterior descending coronary artery [25,26]. Sham-operated and MI rats were then further separated in two subgroups that were sacrificed at 7 days (n=8/group) or 2 months (n= 9 to 11/ group) post-MI. Haemodynamic and echocardiographic measurements were taken 2 months after surgery, followed by heart excision, as previously described[27,28].

Cellular models

H9C2 cells and primary cultures of neonate rat cardiomyocytes (NCM) were prepared and cultured as previously described[29].

Proteomic analysis of plasma samples from REVE-2 patients

Plasma samples underwent no more than two freeze/thaw cycles and were treated combinatorial peptide ligand library (CPLL) method to allow for the enrichment in medium- and low-abundance proteins[30]. 2D-DIGE electrophoresis was performed and analyzed as previously described[31]. Differentially regulated spots were excised manually from a preparative gel performed with 500 µg of proteins and in-gel digested with trypsin[32].

Western blot analysis

The primary antibodies and dilution used for western blot analysis are detailed in the Supplemental Table 1).

Quantification by multiplex immunoassay

B-type natriuretic peptide (BNP) was measured in plasma samples using a Multi Analyte Profiling Kit for simultaneous quantitative detection of rat cardiovascular biomarkers (Rat CVD1 Panel 1, RCVD1-89K Millipore) according to the manufacturer's instructions as previously described[33].

Quantification of clusterin in plasma from REVE-2 and INCA studies

Clusterin was quantified in plasma of REVE-2 patients by western blot. Clusterin was quantified in plasma of INCA patients by LC-MRM MS with SIS peptides and by ELISA (R&D systems, Minneapolis, MN, USA). The endogenous protein concentrations in the patient samples are determined through linear regression[34,35].

Statistical analysis

Data summarized as medians with interquartile range (IQR) were analyzed with GraphPad Prism version 6.01 (GraphPad Software, San Diego, CA). Comparisons were made by Kruskal-Wallis test for REVE-2 and INCA, Wilcoxon-Mann-Whitney test and Wilcoxon- signed rank test for animal and in vitro experiments, as appropriate. Correlations were carried out by Spearman correlation test. Results were considered statistically significant if the $p<0.05$.

RESULTS

Clusterin is increased in patients with high LVR following MI

We performed differential proteomic analysis by comparing 10 pools of 5 patients from the REVE-2 study[9], the pools (1 to 5) and (37-41) corresponding respectively to the lowest (- 17.0 % ± 6.2) and the highest (+ 37.2 % ± 13) LVR (Figure 1A). Because inflammatory response and cytokines are particularly active in early phase after MI, we selected, for each patient pool, the plasma samples collected at 3 months post-MI for the differential 2D-DIGE based proteomic analysis. We found 7 spots differentially expressed (P<0.05) between low and high LVR pooled patients. The MS analyses identified 3 spots as being clusterin (Figure 1B). Detailed 2D-spots corresponding to clusterin are presented for each pool of plasma analyzed (5 for no LVR and 5 for high LVR groups) (Supplemental Figure 1, Supplemental Table 3). We observed that the spots 842, 853 and 873 identified as being clusterin (CLU) gathered as a cluster in this gel within a range of Mw (37-45 kDa) and of pI (4.7-5.0).

To confirm these results, we analyzed CLU plasma levels by 1D-western blotting from individual plasma samples of 45 REVE-2 patients at 3 months post-MI. Patients were divided by tertile of ΔEDV with mean ΔEDV of -7.4% (- 13.9 to 1%) for T1, 11.0% (5.3 to 14%) for T2 and 22.6% (18.7 to 29.5%) for T3. We observed in crude plasma one band with a molecular mass of 36 kDa corresponding to CLU (s-CLU) that is significantly increased in plasma of patients with LVR (P<0.01) (Figure 1C). We also identified clusterin as being significantly increased in plasma from patients with LVR at 1 year post-MI (Supplemental Figure 2).

CLU is increased in the LV of rats after MI and correlated positively with LVR

To determine if increased plasma CLU levels has a cardiac origin, we analyzed CLU expression in the LV of rats at 7 days and 2 months post-MI. In this model, cardiac remodeling was characterized by LV dilatation as shown by significantly increased LV end-diastolic (LVEDD) and end-systolic (LVESD) diameters in the 2 months post-MI rats (Supplemental Table 4). Cardiac hypertrophy was also increased in post-MI: LV weight/Body weight (LVW)/BW) and heart weight (HW)/BW ratios were significantly increased in 2 months post-MI rats (Supplemental Table 4). Also, mRNA levels of ANP and BNP genes were significantly increased in the LV of rats at 7 days and 2 months post-MI (Supplemental Figure 3A) but only BNP plasma levels were significantly increased at 7 days post-MI (Supplemental Figure 3B).

We first analyzed CLU mRNA and its intracellular protein levels in the LV of rats after MI (Figure 2A). Quantitative polymerase chain reaction (qPCR) analysis showed a significant increase of CLU mRNA levels in the LV of rat at 7 days (median [IQR]: 1.7 [1.3-2.7] *vs* 1 [0.8-1.2], P =0.001) and 2 months (1.8 [1.6-2.1] *vs* 1.2 [1.1-1.4], P =0.010) post-MI (Figure 2A, left panel). Western blot analysis detected 2 bands with a molecular mass of 60 and 40 kDa corresponding respectively to the precursor (p-CLU) and the mature (m-CLU) forms of clusterin. The mature form (m-CLU) was the predominant intraventricular form suggesting that CLU maturation is active in the heart independently of MI (Supplemental Figure 3C). We also observed that p-CLU was only significantly increased at 7 days post-MI (0.05 [0.03-0.06] *vs* 0.03 [0.02-0.03], P=0.037) (Figure 2A, middle panel). However, m-CLU was significantly increased at 7 days (0.65 [0.54-0.81] *vs* 0.29 [0.28-0.4], P=0.001) and 2 months post-MI (0.49 [0.37-0.58] *vs* 0.37 [0.31-0.41], P=0.035) compared to the sham-rats (Figure 2A, right panel). However, a significant decrease of p-CLU (0.025 [0.02-0.034] *vs* 0.05 [0.027-0.061], P=0.033) and m-CLU

(0.5 [0.38-0.59] *vs* 0.65 [0.54-0.81], *P*=0.032) levels was observed in the LV of MI rats at 2 months compared to 7 days post-MI (Figure 2A, middle and right panels).

Next, we verified if increased CLU expression in the LV was associated with cardiac remodeling. CLU mRNA level was positively correlated with ANP and BNP expression at 7 days (r=0.76, *P*=0.002 / r=0.85, *P* <0.001, respectively) and 2 months post-MI (r=0.78, *P* <0.001/ r=0.67, *P*=0.004, respectively) (Figure 2B). Cardiac p-CLU and m-CLU levels were positively correlated with plasma BNP levels (r=0.69, *P*=0.004/ r=0.59, *P*=0.018, respectively) at 7 days post-MI (Figure 2C, left panel). The cardiac m-CLU levels were positively correlated with LVEDD (r=0.59, *P*=0.004), LVW/BW ratio (r=0.48, *P*=0.034) and HW/BW ratio (r=0.52, *P*=0.02; data not shown) at 2 months post-MI (Figure 2C, right panel). These data show that CLU expression is increased in LV after MI and is correlated with cardiac remodeling. However, CLU expression is time-dependent after MI, suggesting different mechanisms of CLU regulation and different roles of this protein in cardiac remodeling.

Clusterin expression and secretion are increased in hypertrophied cardiomyocytes

Chronic activation of the adrenergic system with associated up-regulation of the renin–angiotensin–aldosterone (RAA) system plays a major role in cardiac remodeling after MI. To determine the implication of these mechanisms on CLU secretion, we treated H9c2 cells for 48h by Angiotensin II (AII, 2 µmol/L), phenylephrine (PE, 20 µmol/L) and isoproterenol (ISO, 10 µmol/L), agonist of alpha- and beta-adrenergic receptors, respectively. Western blots analysis showed increased s-CLU level in the culture media of H9c2 treated cells compared to untreated cells with the strongest effect with ISO treatment (1.7 [1.1-1.8] *vs* 1, *P* =0.03). The increased s-

CLU level was confirmed at 72h after ISO treatment (2.7 [2-5.3] *vs* 1, *P* =0.02) (Supplemental Figure 4A).

To determine the implication of hypertrophy on CLU regulation, we treated primary cultures of neonatal rat cardiomyocytes (NCM) by ISO (10 µmol/L) for 72h, and characterized cell hypertrophy by increased cell surface area (Figure 3A) and significant increased expression of ANP and BNP genes (Figure 3B). As shown in Figure 3C, the treatment of NCM by ISO increased significantly CLU mRNA level (1.6 [1.1-2] *vs* 1 [0.9-1], *P*=0.01) (left panel), p-CLU level (1.81 [1.46-2.23] *vs* 0.94 [0.9-1.13], *P*<0.001) and m-CLU level (7.85 [6.75-10.9] *vs* 6.43 [5.80-7.83], *P*=0.049) (middle and right panels). Western blot analysis showed increased s-CLU level in culture media of NCM at 72h (1.31 [1.19-1.74] *vs* 0.96 [0.85-1.12], *P*<0.001) after ISO treatment compared to control cells (Figure 3D). These data confirm that CLU expression and secretion are increased by hypertrophied cardiomyocytes and suggest that increased CLU in plasma after MI has at least in part a cardiac origin.

CLU silencing in cardiomyocytes inhibits cell hypertrophy induced by isoproterenol

Since CLU expression and secretion were increased in hypertrophied cardiomyocytes, we studied its role on hypertrophy by silencing it in order to understand its involvement in cardiac remodeling post-MI. We verified that ISO treatment increased significantly phospho Akt (Ser473)/total Akt (pAkt/Akt) ratio, phospho ERK1/2 (Thr202/Tyr204)/total ERK1/2 (pERK1-2/ERK1-2) ratio as previously described[36,37,38] with no significant difference on pGSK-3β (Ser9)/ total GSK-3β (pGSK/GSK) ratio (Supplemental figure 4B). CLU silencing in hypertrophied H9c2 cells (Figure 4A) decreased cell size (Figure 4B) and was associated with significant decreased pERK1/ERK1 (0.79 [0.71-0.9] *vs* 1.01 [0.93-1.07], *P*<0.001) and pERK2/ERK2 (0.87

[0.77-0.98] *vs* 1.01 [0.93-1.07], *P*<0.001) ratios. However, CLU silencing increased significantly pAkt/Akt ratio (1.31 [1.2-1.5] *vs* 0.97 [0.9-1.1], *P* =0.002) with no significant difference on pGSK/GSK ratio (Figure 4C). On another hand, CLU silencing in hypertrophied NCM by using the siRNA-Clu-1 (the first siRNA of pool used in panels A-C) decreased significantly CLU expression (0.24 [0.19-0.34] *vs* 0.8 [0.66-1], *P*<0.001) and CLU secretion (0.04 [0.04-0.07] *vs* 1.02 [0.79-1.21], *P*<0.001) (Figure 4D) and decreased significantly ANP (0.63 [0.41-0.73] *vs* 0.97 [0.84-1.07], *P*<0.001) and BNP (0.35 [0.31-0.55] *vs* 0.7 [0.48-0.87], *P*<0.001) expression (Figure 4E) associated with significantly decreased pERK1/ERK1 (0.74 [0.59-0.85] *vs* 0.95 [0.78-1.19], *P*=0.004) and pERK2/ERK2 (0.56 [0.42-0.72] *vs* 0.98 [0.79-1.21], *P*<0.001) ratios as with the siClu-pool (Figure 4F). These results suggest that CLU silencing inhibits isoproterenol induced hypertrophy by inhibition of ERK1/2 pathway.

CLU is a predictive marker of cardiac mortality in heart failure patients

Since CLU protein levels were higher in the LV of HF rat model than in control rats, we sought to evaluate whether this was also the case in myocardial tissue of HF patients who underwent heart transplantation. We observed an increased level of p-CLU (1.34 [1.17-1.93] *vs* 0.99 [0.87-1.13], *P*=0.009) and m-CLU (5.34 [3.83-7.9] *vs* 2.68 [2.27-3.28], *P*=0.009) in LV of HF patients compared to controls (Figure 5A). Using immunohistochemistry, we also observed an increased CLU staining in failing hearts compared to control hearts with no difference on CLU cellular localization (Figure 5B).

To evaluate whether the secreted form of CLU (s-CLU) may be a predictor of adverse effects in HF patients before heart transplantation, we quantified, by two methods (quantitative mass spectrometry and ELISA), s-CLU in plasma of chronic systolic HF patients (99 alive and 99 dead

patients) from the INCA study recently described[24]. The baseline characteristics of the patients included were matched on age, sex, HF etiology, diabetes. There was no significant difference in treatment at inclusion in the study. The patients who died from a cardiovascular cause during the 3-year follow-up showed significantly higher NYHA class, BNP level, creatinine level, and lower peak VO_2 as compared to patients alive at 3 years. Plasma CLU was increased significantly (73.6 [58.3-82.4] x 10^3 *vs* 30.3 [28.5-73] x 10^3, $P<0.001$ (MS), 150 [103-185] *vs* 134 [99-164], P=0.03 (ELISA) in patients with early cardiac mortality compared to survivors (Figure 5C), independently of HF etiology (not shown).

DISCUSSION

LVR post-MI is associated with an increased risk of HF and death[39]. It remains a frequent event despite the modern therapeutic approach and difficult to predict in clinical practice. For this, we designed the REVE-2 study which included 246 patients after a first anterior MI with serial echocardiography examinations and serial samplings in the first year after MI[9]. Our aim was to identify new biomarkers of LVR post-MI and understand their involvement in this evolutive process.

The development of proteomic analysis techniques makes possible to use new strategies without *a priori* for the identification of proteins involved in cardiovascular pathologies[40]. To identify new biomarkers of LVR post-MI, we performed a differential proteomic analysis, by 2D-DIGE[41], on enriched plasma prepared as previously described[30], obtained from REVE-2 patients with high LVR and patients with no LVR evaluated 1 year after an anterior inaugural MI. We identified several polypeptidic spots corresponding to CLU. The observed molecular mass differences for CLU isoforms in our proteomic study can be explained by the potential N-glycosylation of CLU, consisting of associated complex sugars contributing to 20-30% of its molecular weight[42]. We validated our results by western blot analysis showing that s-CLU isoform with a molecular mass of ~36 kDa is positively associated with high LVR post-MI.

CLU is constitutively expressed in most mammalian tissues and is induced in many organs where tissue injury or remodeling occurs. CLU levels were shown to be increased in plasma of patients after 24h of acute MI[17] and recently described in the exosomes isolated from pericardial fluids collected from MI patients[18]. Our proteomic data is the first study showing that CLU is increased in late stage of MI and is associated with LVR. To verify if increased CLU levels in

plasma (s-CLU) of LVR patients has in part a cardiac origin, we first used an experimental MI rat model[25] in order to analyze the temporal CLU expression in the LV following MI. s-CLU is obtained by proteolytic cleavage of its precursor (p-CLU, 60 kDa) to generate alpha and beta chains of 40 kDa that are glycosylated and assembled to give the mature form, m-CLU that will be then secreted (s-CLU). Our results show that CLU mRNA and its intracellular levels are increased in non-infarcted LV area of MI rat with the mature form as being predominant, suggesting that LV cells are able to express and secrete CLU into the bloodstream. Our results also show that CLU is increased as early as 7 days after MI and correlated with LVR parameters. This finding suggests an implication of CLU in LVR.

To verify if increased CLU expression in the LV is associated with increased CLU secretion, we induced hypertrophy in NCM, a mechanism observed in the non-infarcted area after MI. The 72h-isoproterenol treatment increased CLU expression as shown by its mRNA and intracellular levels. Our results are in agreement with a previous study showing increased CLU levels in the LV of mouse after chronic β-adrenergic stimulation[43]. Interestingly, we also observed increased CLU in the culture media of hypertrophied NCM. All these data show that CLU expression and secretion are increased in hypertrophic cardiomyocytes and suggests that the increased CLU plasma levels in REVE 2 patients with high LVR after MI has, in part, a cardiac origin.

The physiological role of CLU is complex depending on CLU isoforms, localization and cellular types[44]. Several data suggest an anti-apoptotic role of CLU in early phase after MI. In ischemia/reperfusion rat model, the administration of CLU for 3 days reduced both infarct size and death of rats[45]. In addition, infusion of CLU after acute MI reduced the cardiomyocyte apoptosis and increased the induction of epithelial mesenchymal transition, angiogenesis and

preservation of myocardial function[18]. *In vitro*, the addition of CLU in culture media inhibited H9c2 apoptosis induced by ischemic/reperfusion[46]. However, in MI rats, CLU was also detected in peri-infarct zone[47]. These data in addition to our results lead us to study the role of CLU on hypertrophy. In our model, CLU silencing in cardiomyocytes decreased cells size, ANP and BNP expression associated with decreased ERK1/2 activity suggesting a pro-hypertrophic role of CLU in LVR via ERK1/2 pathway. This is supported by previous studies showing, in one hand, a decrease of ERK1/2 pathways after CLU silencing in cancer cells[48] and in another hand, a protective effect of some molecules against hypertrophy via inhibition of ERK1/2 activity[49].

Finally, we validate that CLU expression is also increased in the LV of HF patients that underwent heart transplantation. We evaluated whether the secreted form of CLU may be a predictor of adverse effects in HF patients before heart transplantation, and we showed significantly increased CLU levels in HF patients who died from a cardiovascular cause during the 3-year follow-up compared to survivors, and it is not depending on the HF etiology. However, a recent prognostic study showed a decreased of CLU levels in the plasma of HF patients who died compared to survivors[20]. The discrepancy results observed between the two studies can be explained by a different design of the study. In our case, we performed a case-control study and they included consecutive older HF patients hospitalized, with only 1/3 of the patients with altered ejection fraction (<30% *vs* 100% in our study), a higher female/male ratio and more HF patients with NYHA class III and IV *vs* no class IV patients in our study. A recent study confirmed our data with increased levels of CLU found in circulating extracellular vesicles derived from dilated cardiomyopathy patients compared to controls[50]. As in our study, the patients were relatively young (62.3±11.5 years), mostly men (90%) with reduced ejection

fraction (36.1 ± 11.7) and a ratio NYHA II/III (80/20). Our results suggest that CLU is a new predictive marker of early cardiac mortality.

In conclusion, our data show that CLU is increased in non-infarcted LV at late stage of MI in the rat model. CLU expression is time-dependent in post-MI suggesting different mechanisms of CLU regulation and different roles of this protein in cardiac remodeling. Our data suggest that CLU is involved in the compensatory hypertrophy but its role in HF is not yet elucidated. Since the role of CLU is complex depending on CLU isoforms, localization and cellular types, it will be important to study the mechanisms involved in CLU expression, maturation, secretion and degradation in cardiomyocytes in order to better understand its regulation and its role in different phase after MI. In addition, our study is the first showing that circulating levels of CLU are associated with LVR post-MI and is a new predictive marker of cardiac mortality in HF patients with reduced EF. To consider CLU as a clinically useful biomarker, it should be validated in other cohorts of patients. Our results were obtained in selected patients: 1) with first anterior MI and substantial residual akinesia at predischarge echocardiography; they may not apply to all post-MI patients and; 2) relatively young HF patients with reduced EF. Finally, a gold standard and accurate measurement of CLU usable at hospital should be developed.

WHAT IS NEW?

- This is the first study analyzing the relationship of plasma clusterin levels with left ventricular remodeling following myocardial infarction, discovered by proteomic analysis.

- Our findings suggest that clusterin is involved in compensatory hypertrophy and played a role in early and late phase following myocardial infarction.
- Modulation of plasma clusterin levels is in part of cardiac origin following hypertrophy of cardiomyocytes.
- We show a pro-hypertrophic role of clusterin via ERK1/2 pathway in cardiomyocyte under beta-adrenergic stress.

WHAT ARE THE CLINICAL IMPLICATIONS?

- Despite modern therapeutic approaches, left ventricular remodeling following myocardial infarction remains relatively frequent and difficult to predict in clinical practice.
- Clusterin plasma levels are associated with left ventricular remodeling development following myocardial infarction.
- Our findings suggest that clusterin is involved in compensatory hypertrophy and played a role in early and late phase following myocardial infarction.
- Clusterin plasma levels is new predictive marker of early cardiac mortality in heart failure patients with reduced ejection fraction.
- A significant increase of intracellular clusterin was found in failing human hearts.

SOURCE OF FUNDINGS

This work was supported by grants from the European Union FP7 HOMAGE (305507), French Clinical Research Infrastructure Network INI-CRT (Investigation Network Initiative-

Cardiovascular and Renal Clinical Trialists), and “Agence Nationale de Recherche” 15-CEA-U16/”Direction Ggénérale de l'Offre de Soins” 15-013. Quantitative LC-MRM MS with SIS peptides for clusterin were performed at UVIC-Genome BC Proteomics Centre (Victoria, Canada).

DISCLOSURE

None

REFERENCES

1. Benjamin EJ, Blaha MJ, SE C, Cushman M, Das SR, Deo R, de Ferranti SD, Floyd J, Fornage M, Gillespie C, Isasi CR, Jiménez MC, Jordan LC, Judd SE, Lackland D, Lichtman JH, Lisabeth L, Liu S, Longenecker CT, Mackey RH, Matsushita K, Mozaffarian D, Mussolino ME, P M, Subcommittee. AHASC and SS. Heart Disease and Stroke Statistics-2017 Update: A Report From the American Heart Association. *Circulation*. 2017;135:e146–e603.

2. Jhund PS, Macintyre K, CR S, Lewsey JD, Stewart S, Redpath A, Chalmers JW, Capewell S, McMurray JJ. Long-term trends in first hospitalization for heart failure and subsequent survival between 1986 and 2003: a population study of 5.1 million people. *Circulation*. 2009;119:515–523.

3. Gheorghiade M, Bonow RO. Chronic heart failure in the United States: a manifestation of coronary artery disease. *Circulation*. 1998;97:282–289.

4. St John Sutton M, Pfeffer M, Plappert T, Rouleau J, Moye L, Dagenais G, Lamas G, Klein M, Sussex B, Goldman S, Menapace Jr F, Parker J, Lewis S, Sestier F, Gordon D, McEwan P, Bernstein V, Braunwald E, Lewis J, Sestier F, Gordon D, McEwan P, Bernstein V, Braunwald E, St John Sutton M, Pfeffer MA, Plappert T, Rouleau JL, Moye L, Dagenais G, Lamas G, Klein M, Sussex B, Goldman S. Quantitative two-dimensional echocardiographic measurements are major predictors of adverse cardiovascular events after acute myocardial infarction. The protective effects of captopril. *Circulation*.

1994;89:68–75.

5. de Groote P, Fertin M, Duva Pentiah A, Goeminne C, Lamblin N, Bauters C. Long-Term Functional and Clinical Follow-Up of Patients With Heart Failure With Recovered Left Ventricular Ejection Fraction After -Blocker Therapy. *Circ Heart Fail*. 2014;7:434–439.

6. Erlebacher JA, Weiss JL, Weisfeldt ML, Bulkley BH. Early dilation of the infarcted segment in acute transmural myocardial infarction: role of infarct expansion in acute left ventricular enlargement. *J Am Coll Cardiol*. 1984;4:201–208.

7. Pfeffer M, Braunwald E. Ventricular remodeling after myocardial infarction. Experimental observations and clinical implications. *Circulation*. 1990;81:1161–1172.

8. Savoye C, Equine O, Tricot O, Nugue O, Segrestin B, Sautière K, Elkohen M, Pretorian EM, Taghipour K, Philias A, Aum??geat V, Decoulx E, Ennezat P V., Bauters C. Left Ventricular Remodeling After Anterior Wall Acute Myocardial Infarction in Modern Clinical Practice (from the REmodelage VEntriculaire [REVE] Study Group). *Am J Cardiol*. 2006;98:1144–1149.

9. Fertin M, Hennache B, Hamon M, Ennezat P V., Biausque F, Elkohen M, Nugue O, Tricot O, Lamblin N, Pinet F, Bauters C. Usefulness of Serial Assessment of B-Type Natriuretic Peptide, Troponin I, and C-Reactive Protein to Predict Left Ventricular Remodeling After Acute Myocardial Infarction (from the REVE-2 Study). *Am J Cardiol*. 2010;106:1410–1416.

10. St John Sutton M, Scott CH. A prediction rule for left ventricular dilatation post-MI? *Eur Heart J*. 2002;23:509–511.

11. Braunwald E. Biomarkers in heart failure. Preface. *N Engl J Med*. 2008;5:xiii–xiv.

12. Richards AM, Nicholls MG, Espiner EA, JG L, Troughton RW, J E, C F, Turner J, Crozier IG, Yandle TG. B-type natriuretic peptides and ejection fraction for prognosis after myocardial infarction. *Circulation*. 2003;107:2786–2792.

13. Nagaya N, Nishikimi T, Goto Y, Miyao Y, Kobayashi Y, I M, Daikoku S, Matsumoto T, Miyazaki S, Matsuoka H, Takishita S, Kangawa K, Matsuo H, Nonogi H. Plasma brain natriuretic peptide is a biochemical marker for the prediction of progressive ventricular remodeling after acute myocardial infarction. *Am Heart J*. 1998;31:21–8.

14. Nilsson JC, Groenning BA, G N, Fritz-Hansen T, Trawinski J, Hildebrandt PR, Jensen GB, Larsson HB, Sondergaard L. Left ventricular remodeling in the first year after acute myocardial infarction and the predictive value of N-terminal pro brain natriuretic peptide. *Am Heart J*. 2002;143:696–702.

15. Kelly D, Khan SQ, Thompson M, Cockerill G, Ng LL, Samani N SI. Plasma tissue inhibitor of metalloproteinase-1 and matrix metalloproteinase-9: novel indicators of left ventricular remodelling and prognosis after acute myocardial infarction. *Eur Heart J*. 2008;29:2116–2124.

16. Jones SE, Jomary C. Clusterin. *Int J Biochem Cell Biol*. 2002;34:427–431.

17. Trougakos IP, Poulakou M, Stathatos M, Chalikia A, Melidonis A, Gonos ES. Serum levels of the senescence biomarker clusterin/apolipoprotein J increase significantly in diabetes type II and during development of coronary heart disease or at myocardial infarction. *Exp Gerontol*. 2002;37:1175–1187.

18. Foglio E, Puddighinu G, Fasanaro P, D'Arcangelo D, Perrone GA, Mocini D, Campanella C, Coppola L, Logozzi M, Azzarito T, Marzoli F, Fais S, Pieroni L, Marzano V, Germani A, Capogrossi MC, Russo MA, Limana F. Exosomal clusterin, identified in the pericardial fluid, improves myocardial performance following MI through epicardial activation, enhanced arteriogenesis and reduced apoptosis. *Int J Cardiol*. 2015;197:333–347.

19. Väkevä A, Laurila P, Meri S. Co-deposition of clusterin with the complement membrane attack complex in myocardial infarction. *Immunology*. 1993;80:177–182.

20. Koller L, Richter B, Winter MP, Sulzgruber P, Potolidis C, Liebhart F, Mörtl D, Berger R, G G, Lang I, Wojta J, Hülsmann M, Niessner A. Clusterin/apolipoprotein J is independently associated with survival in patients with chronic heart failure. *J Clin Lipidol*. 2017;11:178–184.

21. de Groote P, Dagorn J, Soudan B, Lamblin N, McFadden E, Bauters C. B-type natriuretic peptide and peak exercise oxygen consumption provide independent information for risk stratification in patients with stable congestive heart failure. *J Am Coll Cardiol*. 2004;43:1584–1589.

22. De Groote P, Lamblin N, Mouquet F, Plichon D, McFadden E, Van Belle E, Bauters C. Impact of diabetes mellitus on long-term survival in patients with congestive heart failure. *Eur Heart J*. 2004;25:656–662.

23. de Groote P, Fertin M, Duva Pentiah A, Goéminne C, Lamblin N, Bauters C. Long-term functional and clinical follow-up of patients with heart failure with recovered left ventricular ejection fraction after beta-blocker therapy. *Circ Heart Fail*. 2014;7:434–439.

24. Lemesle G, Maury F, Beseme O, Ovart L, Amouyel P, Lamblin N, de Groote P, Bauters C, Pinet F. Multimarker proteomic profiling for the prediction of cardiovascular mortality in patients with chronic heart failure. *PLoS One*. 2015;10:e0119265.

25. Mulder P, Devaux B, Richard V, Henry J, Wimart M, Thibout E, Macé B, Thuillez C. Early versus delayed angiotensin-converting enzyme inhibition in experimental chronic heart failure. Effects on survival, hemodynamics, and cardiovascular remodeling. *Circulation*. 1997;95:1314–1319.

26. Pfeffer M, Pfeffer J, Steinberg C, Finn P. Survival after an experimental myocardial infarction: beneficial effects of long-term therapy with captopril. *Circulation*. 1985;72:406–412.

27. Dubois E, Richard V, Mulder P, Lamblin N, Drobecq H, Henry J-P, Amouyel P, Thuillez C, Bauters C, Pinet F. Decreased serine207 phosphorylation of troponin T as a biomarker for left ventricular remodelling after myocardial infarction. *Eur Heart J*. 2011;32:115–123.

28. Mulder P, Barbier S, Chagraoui A, Richard V, Henry JP, Lallemand F, Renet S, Lerebours G, Mahlberg-Gaudin F, Thuillez C. Long-term heart rate reduction induced by the selective I(f) current inhibitor ivabradine improves left ventricular function and intrinsic myocardial structure in congestive heart failure. *Circulation*. 2004;109:1674–1679.

29. Dubois-Deruy E, Belliard A, Mulder P, Bouvet M, Smet-Nocca C, Janel S, Lafont F, Beseme O, Amouyel P, Richard V, Pinet F. Interplay between troponin T phosphorylation and O-N-acetylglucosaminylation in ischaemic heart failure. *Cardiovasc Res*. 2015;107:56–65.

30. Fertin M, Beseme O, Duban S, Amouyel P, Bauters C, Pinet F. Deep plasma proteomic analysis of patients with left ventricular remodeling after a first myocardial infarction. *Proteomics Clin Appl*. 2010;4:654–673.

31. Acosta-Martin AE, Chwastyniak M, Beseme O, Drobecq H, Amouyel P, Pinet F. Impact of incomplete DNase I treatment on human macrophage proteome analysis. *Proteomics Clin Appl*. 2009;3:1236–46.

32. Shevchenko A, Jensen ON, Podtelejnikov AV, Sagliocco F, Wilm M, Vorm O, Mortensen P, Shevchenko A, Boucherie H, Mann M. Linking genome and proteome by mass spectrometry: large-scale identification of yeast proteins from two dimensional gels. *Proc Natl Acad Sci U S A*. 1996;93:14440–14445.

33. Dubois-Deruy E, Belliard A, Mulder P, Chwastyniak M, Beseme O, Henry J-P, Thuillez C, Amouyel P, Richard V, Pinet F. Circulating plasma serine208-phosphorylated troponin T levels are indicator of cardiac dysfunction. *J Cell Mol Med*. 2013;17:1335–44.

34. Percy AJ, Chambers AG, Yang J, Hardie DB, Borchers CH. Advances in multiplexed MRM-based protein biomarker quantitation toward clinical utility. *Biochim Biophys Acta*. 2014;1844:917–926.

35. Mohammed Y, Percy AJ, Chambers AG, Borchers CH. Qualis-SIS: automated standard curve generation and quality assessment for multiplexed targeted quantitative proteomic experiments with labeled standards. *J Proteome Res*. 2015;14:1137–1146.

36. Ueyama T, Kawashima S, Sakoda T, Rikitake Y, Ishida T, Kawai M, Yamashita T, Ishido S, Hotta H, Yokoyama M. Requirement of activation of the extracellular signal-regulated

kinase cascade in myocardial cell hypertrophy. *J Mol Cell Cardiol*. 2000;32:947–960.

37. Yano N, Ianus V, Zhao TC, Tseng A, Padbury JF, Tseng YT. A novel signaling pathway for beta-adrenergic receptor-mediated activation of phosphoinositide 3-kinase in H9c2 cardiomyocytes. *Am J Physiol Heart Circ Physiol*. 2007;293:H385–H393.

38. Chowdhury D, Kumar D, Bhadra U, Devi TA, Bhadra MP. Prohibitin confers cytoprotection against ISO-induced hypertrophy in H9c2 cells via attenuation of oxidative stress and modulation of Akt/Gsk-3β signaling. *Mol Cell Biochem*. 2017;425:155–168.

39. Bauters C, Dubois E, Porouchani S, Saloux E, Fertin M, de Groote P, Lamblin N, Pinet F. Long-term prognostic impact of left ventricular remodeling after a first myocardial infarction in modern clinical practice. *PLoS One*. 2017;12:e0188884.

40. Lindsey ML, Mayr M, Gomes AV, Delles C, Arrell DK, Murphy AM, Lange RA, Costello CE, Jin YF, Laskowitz DT, Sam F, Terzic A, Van Eyk J, Srinivas PR. Transformative Impact of Proteomics on Cardiovascular Health and Disease: A Scientific Statement From the American Heart Association. *Circulation*. 2015;132:852–872.

41. Dupont A, Chwastyniak M, Beseme O, Guihot A-L, Drobecq H, Amouyel P, Pinet F. Application of saturation dye 2D-DIGE proteomics to characterize proteins modulated by oxidized low density lipoprotein treatment of human macrophages. *J Proteome Res*. 2008;7:3572–82.

42. Burkey BF, de Silva HV, Harmony JAK. Intracellular processing of apolipoprotein J precursor to the mature heterodimer. *J Lipid Res*. 1991;32:1039–1048.

43. Dostanic S, Servant WC, Wang C, Chalifour LE. Chronic beta-adrenoreceptor stimulation

in vivo decreased Bcl-2 and increased Bax expression but did not activate apoptotic pathways in mouse heart. *Can J Physiol Pharmacol*. 2004;82:167–174.

44. Rohne P, Prochnow H, Koch-Brandt C. The CLU-files: disentanglement of a mystery. *Biomol Concepts*. 2016;7:1–15.

45. Van Dijk A, Vermond RA, Krijnen PAJ, Juffermans LJM, Hahn NE, Makker SP, Aarden LA, Erik H, Spreeuwenberg M, van Rossum BC, Meischl C, Paulus WJ, Van Milligen FJ, Niessen HWM. Intravenous clusterin administration reduces myocardial infarct size in rats. *Eur J Clin Invest*. 2010;40:893–902.

46. Krijnen PAJ, Cillessen SAGM, Manoe R, Muller A, Visser CA, Meijer CJLM, Musters RJP, Hack CE, Aarden LA, Niessen HWM. Clusterin: a protective mediator for ischemic cardiomyocytes? *Am J Physiol Heart Circ Physiol*. 2005;289:H2193–202.

47. Silkensen JR, Hirsch AT, Lunzer MM, Chmielewski D, Manivel JC, Muellerleile MR, Rosenberg ME. Temporal induction of clusterin in the peri-infarct zone after experimental myocardial infarction in the rat. *J Lab Clin Med*. 1998;131:28–35.

48. Tang Y, Liu F, Zheng C, Sun S, Jiang Y. Knockdown of clusterin sensitizes pancreatic cancer cells to gemcitabine chemotherapy by ERK1/2 inactivation. *J Exp Clin Cancer Res*. 2012;31:73.

49. Song Y, Xu J, Li Y, Jia C, Ma X, Zhang L, Xie X, Zhang Y, Gao X, Zhang Y, Zhu D. Cardiac ankyrin repeat protein attenuates cardiac hypertrophy by inhibition of ERK1/2 and TGF-β signaling pathways. *PLoS One*. 2012;7:e50436.

50. Roura S, Gamez-Valero A, Lupon J, Galvez-Monton C, Borras F, Bayes-Genis A.

Proteomic signature of circulating vesicles in dilated cardiomyopathy. *Lab Investig*. 2018; 14 Mar doi: 10.1038/s41374-018-0044-5. [epub ahead of print].

FIGURE LEGENDS

Figure 1: Discovery of clusterin as biomarker of high LVR by differential 2D-DIGE proteomic analysis. A: Constitution of pooled patients according to the increasing percent of LVR. Five pools with the lowest (1-5) and the highest (37-41) percent of LVR were used for the 2D-DIGE analysis after treatment of pooled plasma by the CPLL method as previously described [30]. **B**: Representative 2D-DIGE gel and bioinformatic analysis of spots surrounded corresponding to clusterin in pooled plasma of patients with the lowest and highest percent of LVR at 3 months post-MI. **C**: Representative western blot (left panel) and quantification (right panel) of clusterin (s-CLU) in plasma of 45 REVE-2 patients at 3 months post-MI. Patients were divided by tertile of ΔEDV (n=15 per tertile), with mean ΔEDV of -7.4% (- 13.9 to 1%) for T1, 11.0% (5.3 to 14%) for T2 and 22.6% (18.7 to 29.5%) for T3. M: size marker, S: standard added in each 1D-gel performed for normalization between gels. Red ponceau was used to normalize clusterin levels. Data are expressed in arbitrary unit (A.U.) and presented as box and whisker plots showing median (line) and min to max (whisker). Statistical significance was determined by Kruskal-Wallis test. ** $P<0.01$.

Figure 2: Clusterin expression is increased in the left ventricle after MI and correlated positively with LVR parameters. **A**: Analysis of clusterin expression in LV of sham and MI-rats at 7 days and 2 months after ligation. Quantification, by RT-qPCR, of clusterin (CLU) mRNA levels (left panel) in the LV of sham- and MI- rats at 7 days (n=8/group) and 2 months (n=9/group) post-MI. HPRT was used to normalize CLU expression. Representative western blots and quantification of intraventricular levels of precursor (p-CLU, middle panel) and mature (m-CLU, right panel) forms of clusterin at 7 days (n=8/group) and 2 months (n=11/group) post-

MI. GAPDH was used to normalize CLU levels. Data are expressed in arbitrary unit (A.U.) and presented as box and whisker plots showing median (line) and min to max (whisker). Statistical significance was determined by Wilcoxon-Mann Whitney test. *P<0.05, **P<0.01 *vs* Sham rats and $^{\#}P$<0.05 *vs* 7 days. **B**: Correlation of CLU mRNA with ANP (atrial natriuretic peptide) and BNP (brain natriuretic peptide) mRNAs in LV of MI rats at 7 days (left panels, n=14) and 2 months post-MI (right panels, n=17). **C**. Correlation of intraventricular clusterin (p-CLU or m-CLU) with BNP plasma levels at 7 days post-MI (left panels, n=16), and with LV weight/ body weight ratio (LVW/BW) and with LV end diastolic diameter (LVEDD) at 2 months post-MI (right panels, n=21). Statistical significance was determined by Spearman correlation test.

Figure 3: Clusterin expression and secretion are increased in hypertrophied cardiomyocytes. The isolated rat neonatal cardiomyocytes (NCM) were cultured in 1% SVF medium without (cont.) or with 10 µmol/L of isoproterenol (ISO) for 72 hours. **A**: Representative control- and ISO-treated cells observed by phase-contrast (upper panels) and fluorescence microscopy after incubation with cell Mask red plasma membrane stain (lower panels), nuclei are stained in blue by DAPI. **B**: RT-qPCR analysis of cardiac hypertrophic markers genes (ANP and BNP) in the ISO-treated cells (n=9) compared to control cells (n=7). GAPDH was used to normalize ANP and BNP expression and data are expressed in arbitary units (A.U.). **C**: Analysis of CLU expression in NCM after ISO treatment. Quantification by RT-qPCR, of CLU mRNA levels (left panel) in the ISO-treated cells (n=9) compared to control cells (n=7). GAPDH was used to normalize CLU expression and data are expressed in arbitary units (A.U.). Representative western blot (middle panel) and quantification (right panel) of intracellular levels of precursor (p-

CLU) and mature (m-CLU) forms of clusterin in the ISO-treated cells (n=13) compared to control cells (n=13). Sarcomeric actin (S-Actin) was used to normalize intracellular CLU levels and data are expressed in fold change in CLU levels relative to p-CLU of control cells. **D**: Representative western blot (left panel) and quantification (right panel) of secreted CLU levels (s-CLU) in the culture media of NCM treated by ISO (n=19) compared to control cells (n=18). Red ponceau (RP) was used to normalize secreted CLU levels and data are expressed in fold change in CLU levels relative to control cells. All data are presented as box and whisker plots showing median (line) and min to max (whisker). Statistical significance was determined by Wilcoxon-Mann Whitney test and by Wilcoxon signed rank test. **P*<0.05, ***P*<0.01, ****P*<0.001 *vs* control cells and $^{\#\#\#}P$<0.001 *vs* p-CLU.

Figure 4: Clusterin silencing inhibited cardiomyocytes hypertrophy induced by isoproterenol. The H9c2 cells and NCM were transfected by siRNA non target (si-NT) used as control or siRNA targeting clusterin (si-Clu pool [siRNA 1 to 4] for H9c2 cells and si–Clu 1 [siRNA 1] for NCM) 24h before treatment by isoproterenol (ISO) for 72h. **A**: Representative western blot of s-CLU levels in the culture media of H9c2 cells after CLU silencing (si-Clu pool) compared to si-NT transfected cells. **B**: Cell mask plasma membrane staining of H9c2 cells after CLU silencing (si-Clu pool) compared to si-NT transfected cells treated or no by ISO. Nuclei are stained in blue by DAPI. **C**: Representative western blot (left panels) and quantification (right panels), of active form (phosphorylated/total ratio) of Akt, GSK-3β and ERK1/2, in the H9c2 cells after CLU silencing (si-Clu pool) compared to si-NT transfected cells (n=12/group). Data are expressed in fold change in active proteins levels relative to si-NT transfected cells. **D**: Quantification by RT-qPCR of CLU mRNA (left panel) and by western blot, of s-CLU levels in

the culture media (right panel) of NCM after CLU silencing (si-Clu 1) compared to si-NT transfected cells (n=11/group). For RT-qPCR analysis, GAPDH was used to normalize CLU expression and the data are expressed in arbitary units (A.U.). For western blot analysis, red ponceau (RP) was used to normalize s-CLU levels and the data are expressed in fold change relative to si-NT transfected cells. **E**: Quantification by qPCR, of ANP (left panel) and BNP (right panel) expression in the NCM cells after CLU silencing (si-Clu 1) compared to si-NT transfected cells (n=17/group). GAPDH was used to normalize ANP and BNP expression and data are expressed in arbitary units (A.U.). **F**: Representative western blots (left panels) and quantification (right panels) of active form of ERK1/2 (pERK1/ERK1 and pERK2/ERK2) in the NCM after CLU silencing (si-Clu 1) compared to si-NT transfected cells (n=19/group). Data are expressed in fold change in active proteins levels relative to si-NT transfected cells. All data are presented as box and whisker plots showing median (line) and min to max (whisker). Statistical significance was determined by Wilcoxon- Mann Whitney test. **P*<0.05, ***P*<0.01, ****P*<0.001 *vs* si-NT transfected cells.

Figure 5: Clusterin protein levels in human myocardial and plasma samples from HF patients. A: Western Blot and quantification of clusterin precursor (p-CLU) and its mature form (m-CLU) levels in LV biopsies obtained from non-failing controls (cont.) or heart failure (HF) patients with ischemic dilated cardiomyopathy (n=6/group). ↑: indicate the samples used for immunostaining in B. GAPDH was used to normalize intracellular CLU levels. Graphs show individual and median fold change in CLU levels ± IQR (25%-75%) relative to p-CLU of control. **B:** Immunostaining of CLU in frozen myocardial sections from non-failing (control) and heart failure (HF) patients with ischemic cardiomyopathy. Nuclei are stained in blue by

hematoxylin. **C:** Quantification of s-CLU plasma levels in systolic HF patients alive (n=99) or dead (n=99) within 3 years after the initial prognostic evaluation by quantitative mass spectrometry (left panel) and ELISA (right panel). Data are presented as box and whisker plots showing median (line) and min to max (whisker). Statistical significance was determined by Wilcoxon-Mann Whitney test or and by Wilcoxon signed rank test. $^{**}P<0.01$ *vs* Cont., $^{\#}P<0.05$ *vs* p-CLU (**A**), $^{*}P<0.05$, $^{***}P<0.001$ *vs* alive patients (**C**).

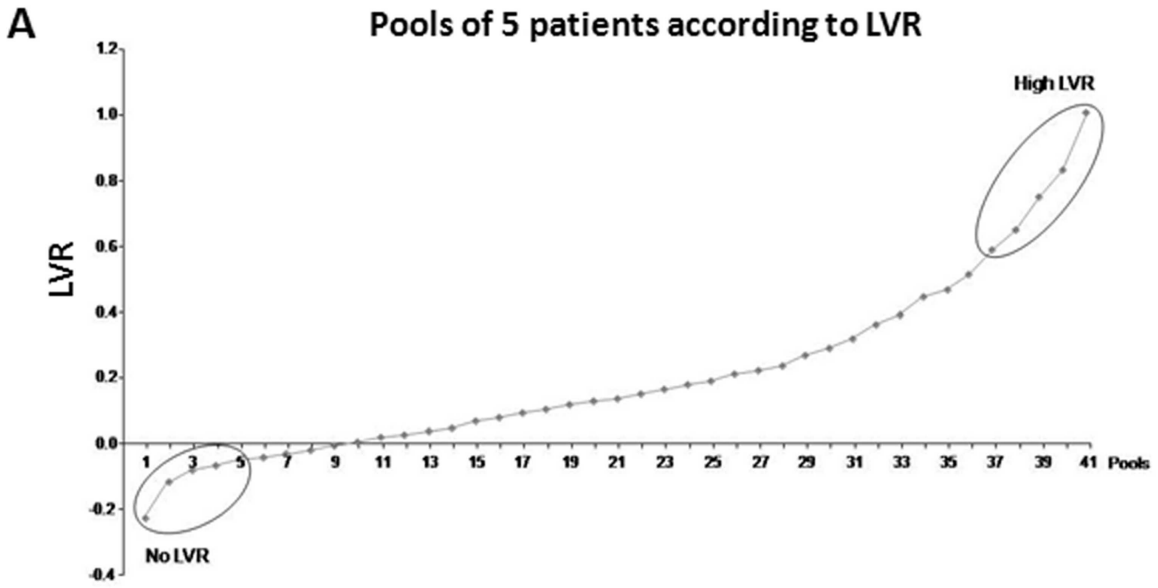

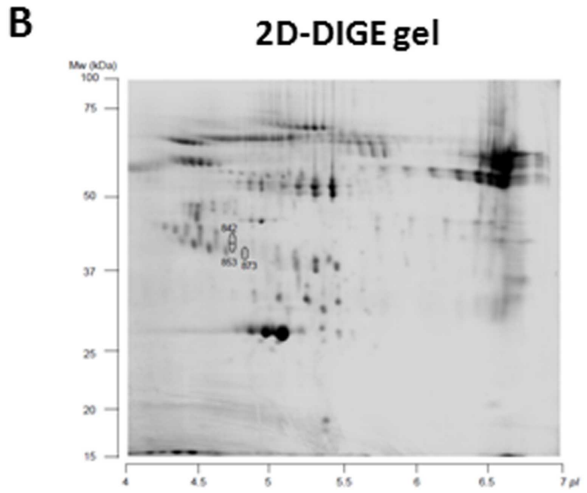

Differential proteomic analysis

Spot	Fold	*P*-value
842	1.3	0.017
853	1.5	0.031
873	1.3	0.043

Clusterin (P10909)

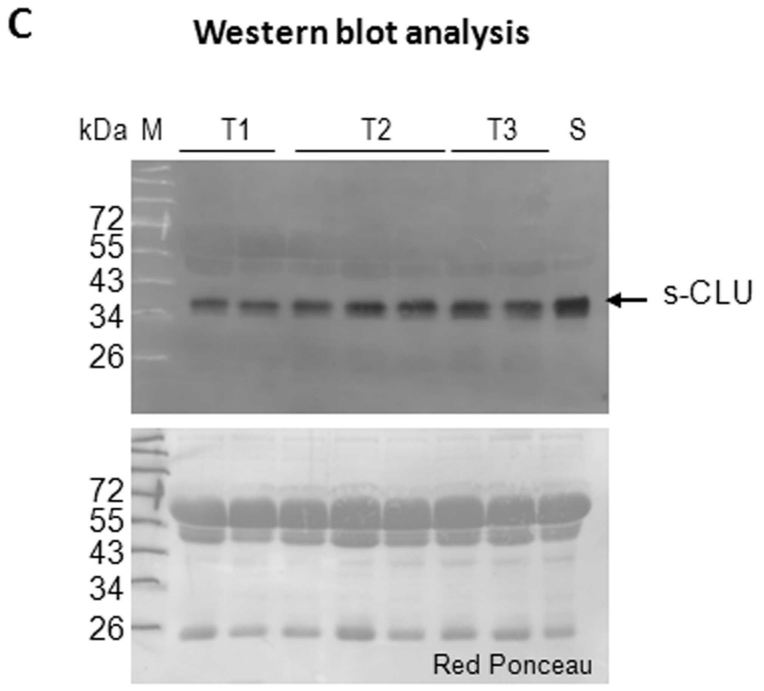

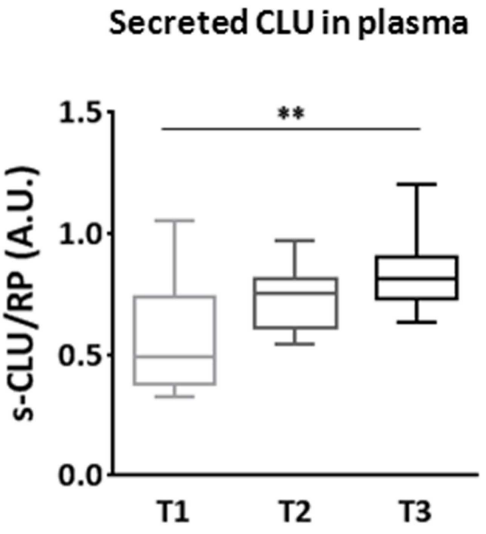

Figure 1

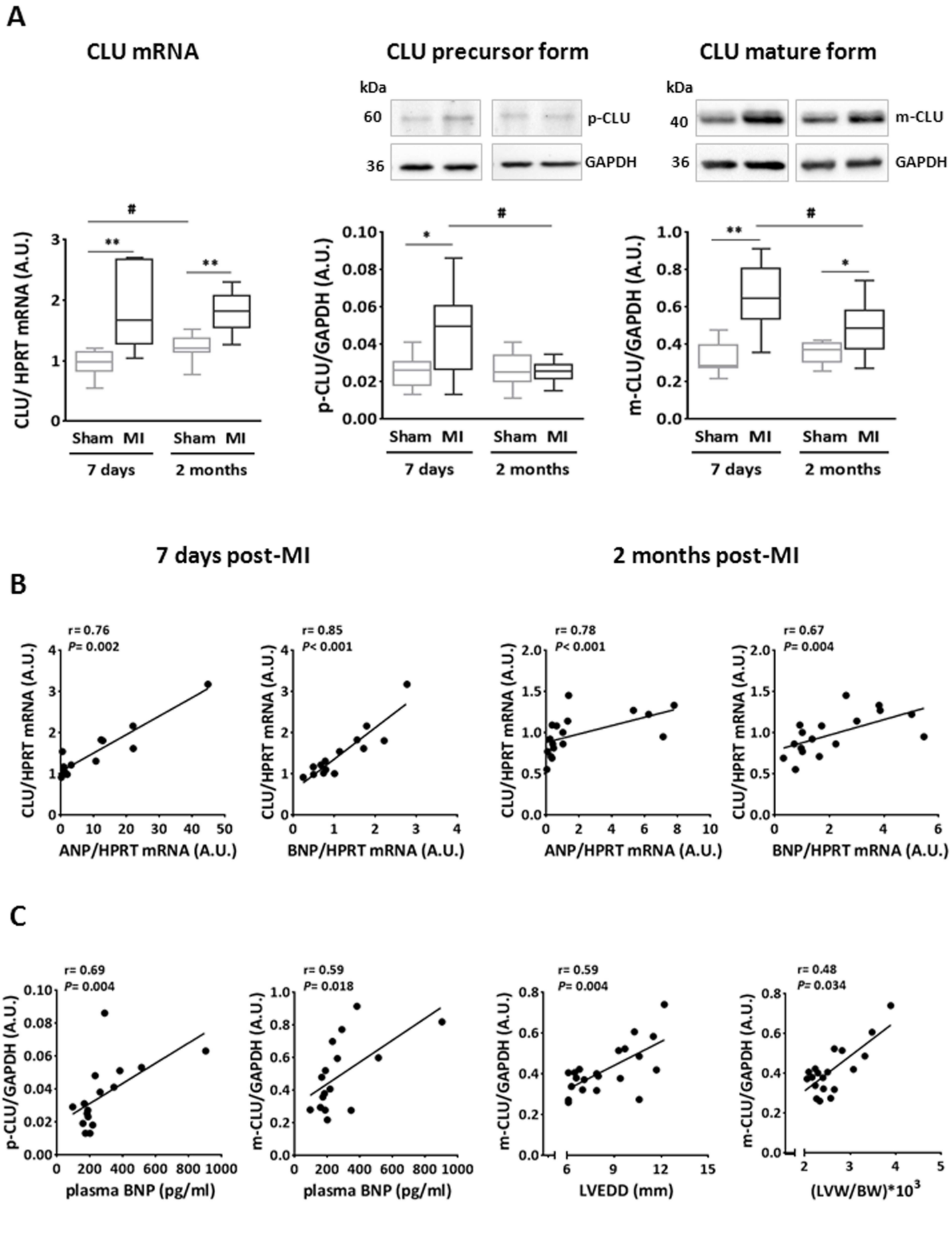
A
CLU mRNA
CLU precursor form
CLU mature form
kDa
60
p-CLU
36
GAPDH
kDa
40
m-CLU
36
GAPDH
CLU/ HPRT mRNA (A.U.)
p-CLU/GAPDH (A.U.)
m-CLU/GAPDH (A.U.)
Sham MI Sham MI
7 days 2 months
B
7 days post-MI
2 months post-MI
r= 0.76
P= 0.002
r= 0.85
P< 0.001
r= 0.78
P< 0.001
r= 0.67
P= 0.004
CLU/HPRT mRNA (A.U.)
ANP/HPRT mRNA (A.U.)
BNP/HPRT mRNA (A.U.)
C
r= 0.69
P= 0.004
r= 0.59
P= 0.018
r= 0.59
P= 0.004
r= 0.48
P= 0.034
p-CLU/GAPDH (A.U.)
m-CLU/GAPDH (A.U.)
plasma BNP (pg/ml)
LVEDD (mm)
(LVW/BW)*10^3

Figure 2

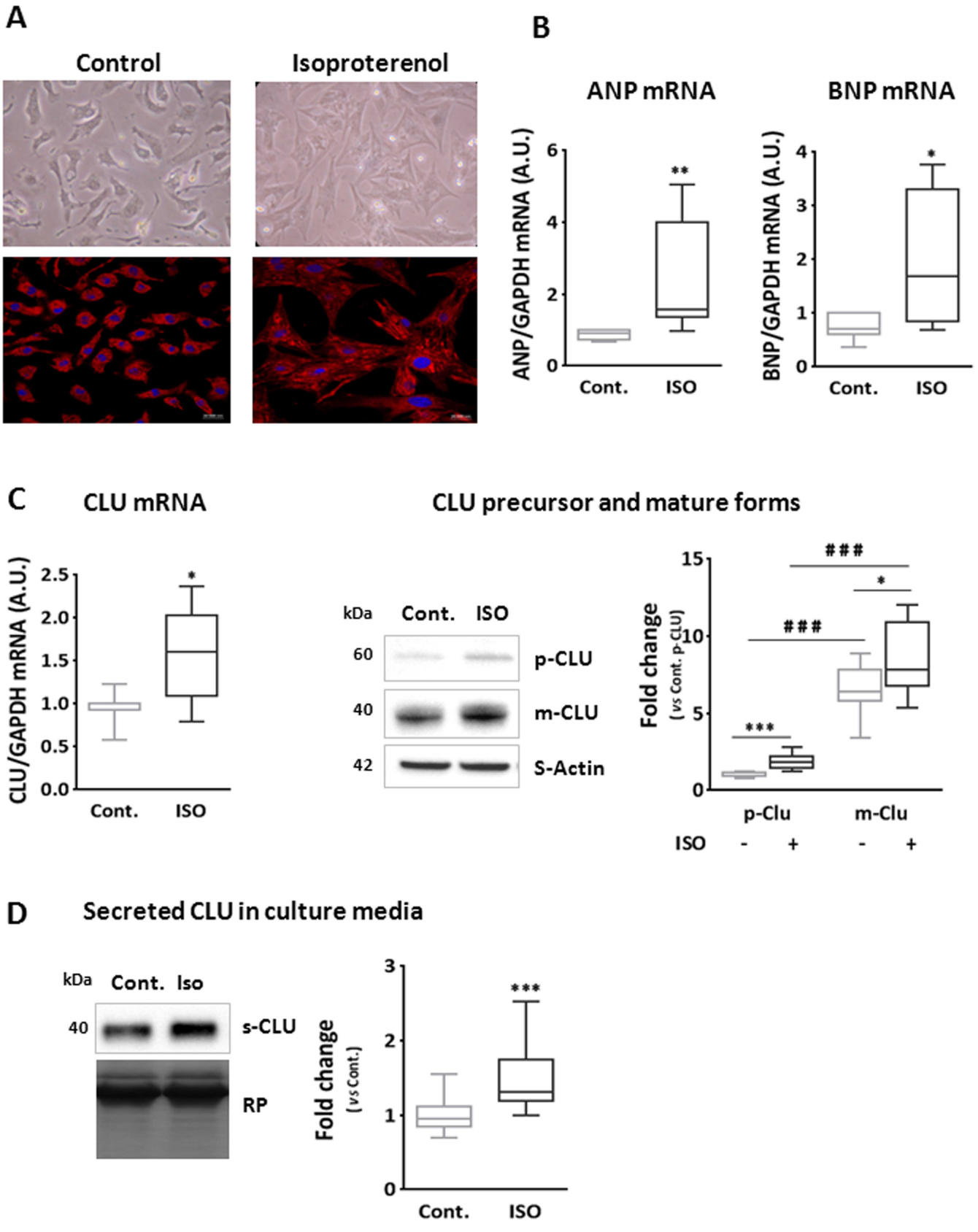
A
Control
Isoproterenol
B
ANP mRNA
BNP mRNA
ANP/GAPDH mRNA (A.U.)
BNP/GAPDH mRNA (A.U.)
Cont.
ISO
C
CLU mRNA
CLU precursor and mature forms
CLU/GAPDH mRNA (A.U.)
kDa
Cont.
ISO
60
40
42
p-CLU
m-CLU
S-Actin
Fold change
(vs Cont. p-CLU)
p-Clu
m-Clu
ISO
D
Secreted CLU in culture media
Iso
s-CLU
RP
Fold change
(vs Cont.)

Figure 3

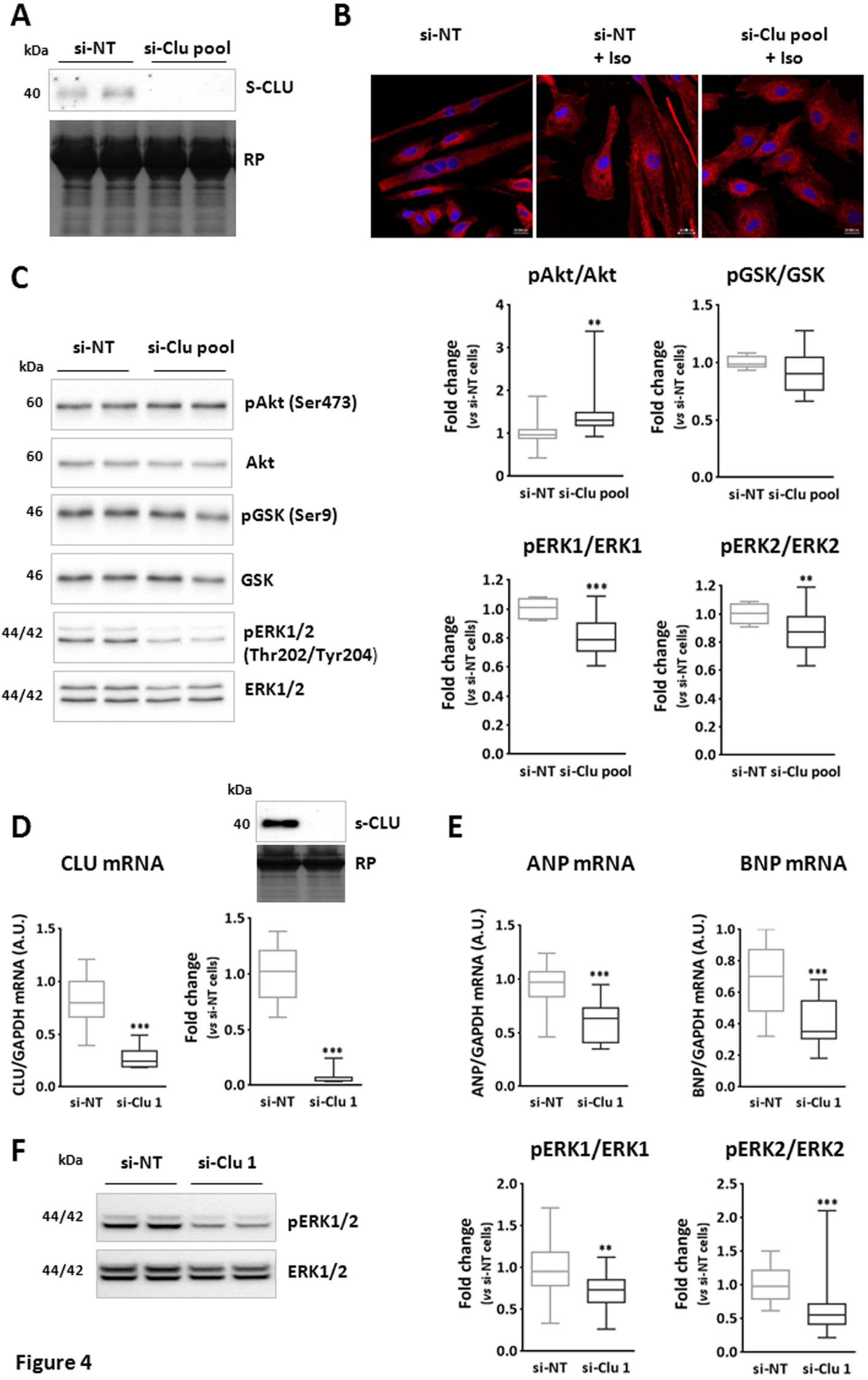
A
kDa
si-NT
si-Clu pool
40
S-CLU
RP
B
si-NT
si-NT + Iso
si-Clu pool + Iso
C
si-NT
si-Clu pool
kDa
60
pAkt (Ser473)
60
Akt
46
pGSK (Ser9)
46
GSK
44/42
pERK1/2 (Thr202/Tyr204)
44/42
ERK1/2
pAkt/Akt
pGSK/GSK
pERK1/ERK1
pERK2/ERK2
Fold change (vs si-NT cells)
si-NT si-Clu pool
D
kDa
40
s-CLU
RP
CLU mRNA
CLU/GAPDH mRNA (A.U.)
Fold change (vs si-NT cells)
si-NT
si-Clu 1
E
ANP mRNA
BNP mRNA
ANP/GAPDH mRNA (A.U.)
BNP/GAPDH mRNA (A.U.)
F
kDa
si-NT
si-Clu 1
44/42
pERK1/2
44/42
ERK1/2
pERK1/ERK1
pERK2/ERK2

Figure 4

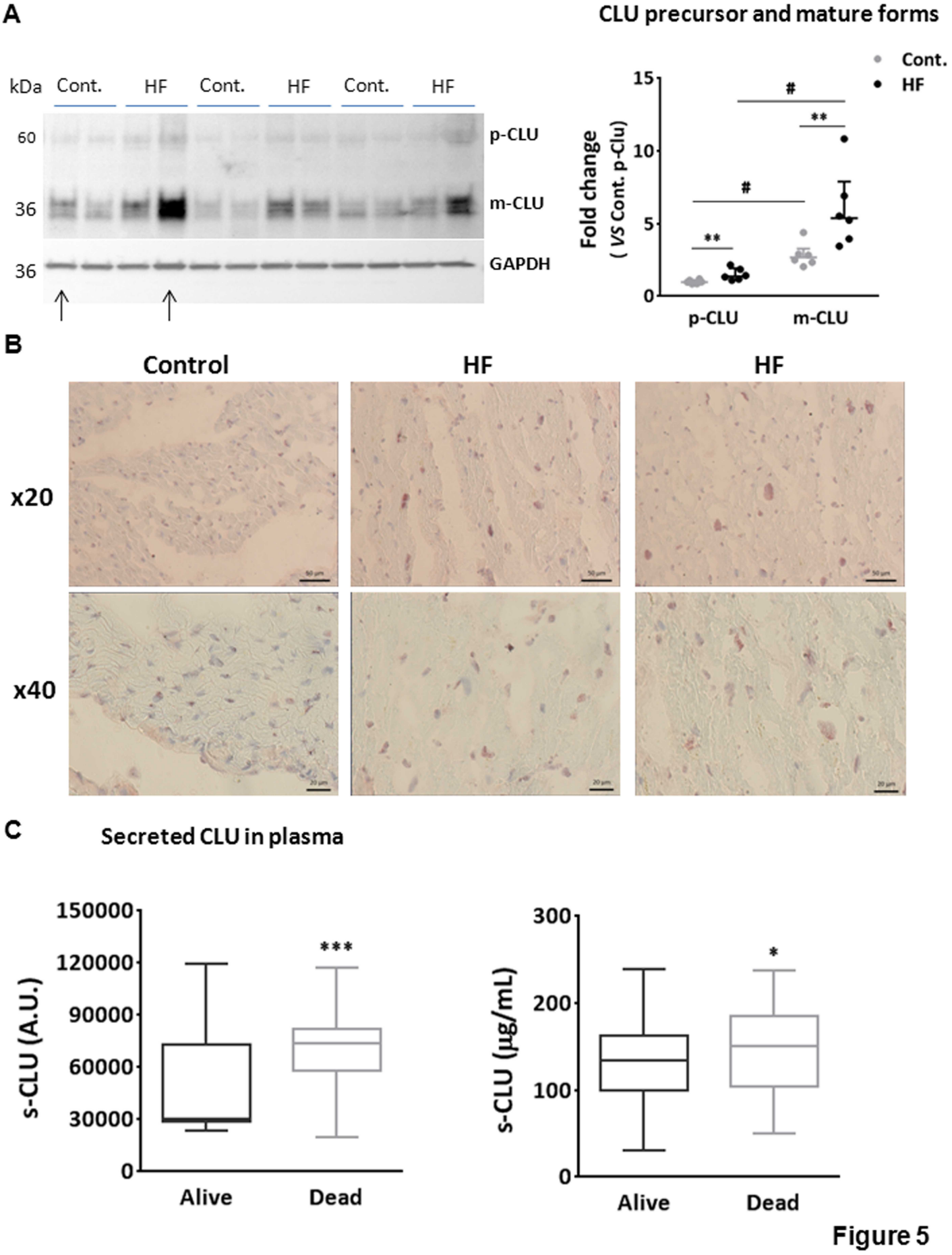
A
CLU precursor and mature forms
kDa
Cont.
HF
Cont.
HF
Cont.
HF
60
36
36
p-CLU
m-CLU
GAPDH
Cont.
HF
Fold change
(VS Cont. p-Clu)
15
10
5
0
#
**
#
**
p-CLU
m-CLU
B
Control
HF
HF
x20
x40
C
Secreted CLU in plasma
s-CLU (A.U.)
150000
120000
90000
60000
30000
0
***
Alive
Dead
s-CLU (µg/mL)
300
200
100
0
*
Alive
Dead

Figure 5

CIRCHF/2017/004838-R2

SUPPLEMENTAL DATA

Expression and implication of clusterin in left ventricular remodeling after myocardial infarction

Annie Turkieh, PhD[a], Marie Fertin, MD, PhD[a], Marion Bouvet, PhD[a], Paul MulderPhD[b], Hervé Drobecq, MSC[c], Gilles Lemesle, MD, PhD[a,d,e,f], Nicolas Lamblin, MD, PhD[a,d,e,f], Pascal de Groote, MD, PhD[a,d], Sina Porouchani, MSC[a], Maggy Chwastyniak, MSC[a], Olivia Beseme, MSC[a], Philippe Amouyel, MD, PhD[a,e,g], Frédéric Mouquet, MD, PhD[d], Jean-Luc Balligand, MD, PhD[h], Vincent Richard, PhD[b], Christophe Bauters, MD[a,d,e,f], Florence Pinet, PhD[a]

EXPANDED MATERIALS AND METHODS

Patients

The studies were approved by the Ethics Committee of the "Centre Hospitalier et Universitaire de Lille" and comply with the Declaration of Helsinski. All patients gave written informed consent.

REVE-2 study

The design of the REVE-2 study has been published in detail elsewhere[1]. We enrolled 246 patients with a first anterior wall Q-wave MI between February 2006 and September 2008. Inclusion criteria were hospitalization within 24 hours after symptom onset and at least 3 akinetic LV segments in the infarct zone at the predischarge echocardiography. The protocol required serial echographic studies at baseline (day 3 to day 7) and 3 and 12 months after MI. Serial blood samples were taken at baseline (day 3 to day 7), and 1, 3, and 12 months after MI.

A standard echographic imaging protocol was used based on apical 4- and 2-chamber views. All echocardiograms were analyzed at the Lille Core Echo Laboratory (Lille, France), as previously described[1]. LV end-diastolic volume (EDV), LV end-systolic volume (ESV), and LV ejection fraction (EF) were calculated with a modified Simpson's rule. Left ventricular remodeling (LVR) was defined as percent change in EDV from baseline to 1 year.

Blood samples were collected in EDTA-containing tubes. Plasma was obtained by centrifugation at 800g for 10 min. Samples were aliquot, and stored at −80 °C until further analysis.

INCA study

All patients referred for evaluation of systolic HF (LVEF <45%) in our institution between November 1998 and May 2010 were included in a prospective cohort on prognostic indicators [2,3,4,5]. All patients were ambulatory and clinically stable for at least 2 months, and received

optimal medical therapy with maximal tolerated doses of angiotensin-converting enzyme inhibitors and betablockers. At inclusion, patients underwent a prognostic evaluation including: BNP level assessment, echocardiography, and cardiopulmonary exercise testing as previously described[2,4]. In addition, patients underwent a coronary angiogram to help define the etiology of left ventricular (LV) systolic dysfunction as either ischemic or nonischemic. A follow-up was performed at 3 years to assess clinical outcome. All events were adjudicated by two investigators and by a third one in case of disagreement. Cardiovascular death included cardiovascular-related death, urgent transplantations defined as United Network for Organ Sharing (UNOS) status 1), and urgent assist device implantation.

From this population, we selected 198 patients included between November 1998 and December 2005. Ninety nine patients who died from cardiovascular cause within 3 years after the initial prognostic evaluation (cases) were individually matched for age, sex, and HF etiology with 99 patients who were still alive at 3 years (controls) as previously described[6].

At inclusion, peripheral blood was collected in tubes containing EDTA and plasma samples were stored at -80°C.

Human heart biopsies

Tissues from failing and non-failing human hearts were obtained respectively from Lille University Hospital (France) and from Catholic University of Leuven (Belgium). Explanted heart tissues were obtained from patients undergoing heart transplantation for end-stage ischemic heart failure and from patients died of non-cardiac causes. Samples were quick-frozen and stored at -80°C. All materials from patients and controls were recovered as surgical waste with informed consent of the donors and with approval of the local ethical boards and according to the Declaration of Helsinki.

Animal models

All animal experiments were performed according to the Guide for the Care and Use of Laboratory Animals published by the US National Institutes of Health (NIH publication NO1-OD-4-2-139, revised in 2011). Animals were used and experimental protocols performed under the supervision of a person authorized to perform experiments on live animals (F. Pinet: 59-350126). Approval was granted by the institutional ethics review board (CEEA Nord Pas-de-Calais N°242011, January 2012).

Before surgery, rats were anaesthetized (sodium methohexital, 50 mg/kg intraperitoneally (IP)), while analgesia was administered before (xylazine 5 mg/kg IP) and 1 hr after surgery (xylazine 50 mg/kg subcutaneously) as described [7]. Anesthesia and sedation were controlled by monitoring heart rate. MI was induced in 10-week-old male Wistar rats (Janvier, Le Genest St isle, France) by ligation of the left anterior descending coronary artery[7,8]. Sham-operated and MI rats were then further separated in two subgroups that were sacrificed at 7 days (n=8/group) or 2 months (n= 9 to 11/ group) post-MI. Haemodynamic and echocardiographic measurements were taken 2 months after surgery, followed by heart excision, as previously described[9,10].

Cellular models

H9C2 cells

Rat cardiac myoblasts (H9c2 cells, CRL-14146, ATCC) were cultured in Dulbecco's Modified Eagle's Medium (DMEM Glutamax, 31966, Gibco, Life Technologies) with addition of 10% (v/v) fetal bovine serum (FBS, 30-2020, ATCC) and 1% penicillin and streptomycin (P/S, 10,000 U/mL) (15140-122, Invitrogen™, Life Technologies). Cells were cultured at 37°C under 5% CO_2 atmosphere.

Primary cultures of neonate rat cardiomyocytes (NCM)

Primary cultures of rat neonatal contractile cardiac myocytes (NCMs) were prepared from heart ventricles of 1- or 2-day-old rats, killed by decapitation, minced in a balanced salt solution containing 20 mmol/L HEPES, 120 mmol/L NaCl, 1 mmol/L NaH_2PO_4, 5.5 mmol/L glucose, 5.4 mmol/L KCl, and 0.8 mmol/L $MgSO_4$ [pH 7.4] and then digested by using pancreatin and collagenase type II as previously described[11]. NCMs were purified by centrifugation of the cells at 2800 rpm for 30 min on Percoll gradients (58.5% and 40.5% in the balanced salt solution). NCMs were seeded at a density 6.5×10^5 cells/well in 6-well plates coated with 10% of collagen (Sigma-Aldrich) and cultured in a medium containing 4 parts of Dulbecco's modified Eagle's medium (DMEM, D1152, Sigma-Aldrcih) and 1 part of Medium199 (M199, M2520, Sigma), 10% FBS and 1% P/S at 37°C under 5% CO_2 atmosphere.

Hypertrophic treatment

After 24h of seeding, cells were serum deprived for 24 h and then treated with isoproterenol (10 µmol/L, Tocris Bioscience, 1747), Angiotensin II (2 µmol/L, A9525, Sigma-Aldrich) or phenylephrine (20 µmol/L, 2838, Tocris Bioscience) for 48 h or 72h in the presence of 1% FBS.

Transfection studies

To inhibit the expression of Clusterin, cells were transfected by 25 nmol/L of siRNA non target (D-001810-10-20, Dharmacon) as a control or ON-TARGETplus Rat Clu siRNA (Smart pool, or the first individual siRNA, Dharmacon) using Darmaphect according to the manufacturer's instructions. For treatment of transfected cells with isoproterenol, the transfection was occurred in serum and P/S free medium 24h before the treatment.

Immunostaining studies

Immunohistochemistry

Frozen human heart tissues were included in Richard-Allan Scientific Neg-50^{TM} (ThermoFisher Scientific). Tissue Sections (5 µm thickness) were fixed with acetone/methanol (V:V) for 20 min at -20°C. The endogenous peroxidase activity was blocked in 0.3% hydrogen peroxide (H_2O_2) in methanol for 30 min at room temperature. After washing with TN (Tris 2.42 g/L and NaCl 29.22 g/L in water), the sections were saturated with TNO (TN with ovalbumin at 5 g/L) for 30 min at room temperature and then incubated with polyclonal rabbit clusterin antibody (ab42673, Abcam) diluted at 1/50 in TNO overnight at 4°C. After washing with TNO, Sections were incubated with anti-rabbit biotinylated secondary antibody (BA-1000, Vector laboratories) diluted at 1/200 in TNO for 1h at room temperature, washed and then incubated in Vectastain Elite ABC Kit (vector laboratories) for 30 min. Finally the sections were developed in ABC staining kit (sigma) for 5 min, counter-stained with hematoxylin to identify nuclei and mounted in glycerol. Staining was visualized with the x20 and x40 objectives of color Axioplan 2 microscope followed by Zen image acquisition.

Immunofluorescence

For measuring cell surface area, the cells were plated at a density of 2 x 10^5 cells on coverslip (24 mm x 24 mm) for H9c2 cells and 8x10^8 cells on coverslip coated with collagen for NCM in a 6-wells culture plate. After treatment, the cells were incubated with the complete medium containing Hoechst (33342, Invitrogen) for 30 min at 37°C to color nuclei, then with the Cell Mask plasma membrane stain (C10046, Life Technology) at a final concentration of 1X in the medium for 10 min at 37°C. The cells were then fixed with 3.75 % paraformaldehyde (43368, Thermofisher) for 10 min at room temperature and then wash three times for 5 min with PBS 1X. The coverslips were mounted on slides with glycerol 90%. Staining was visualized with the x40 objectives of LSM710 confocal microscope followed by Zen image acquisition.

Proteomic analysis of plasma samples from REVE-2 patients

Constitution of pooled plasma samples

The follow-up of REVE-2 study was completed for 205/246 patients (serial echography and blood samples). The 205 patients were ranked by the increasing percentage of LVR, and then grouped together by 5, defining 41 pools. The pools with the lowest (1 to 5) and with the highest (37-41) percent of LVR were constituted by mixing an equal volume of plasma from the 5 patients in the same group (Figure 1A).

Processing of pooled plasma

Prior to the proteomic study, plasma samples underwent no more than two freeze/thaw cycles. One mL of each plasma sample was treated with the ProteoMiner™ kit (Bio-Rad Laboratories, Hercules, CA, USA) as previously described[12,13]. This combinatorial peptide ligand library (CPLL) method has been shown to be reproducible and to allow for the enrichment in medium- and low-abundance proteins[14]. Samples were eluted by adding 100 µL elution reagent, repeated three times and the pooled samples were stored at −20°C, before the protein concentration was determined for 2D analysis.

2D-DIGE electrophoresis

Two gels (technical replicates) of each sample were run with a total of 10 µg of mixed labelled protein per gel. These protein mixtures contained 5 µg of protein from each REVE 2 sample group (pool of 4 patients and pool of 4 healthy donors) randomly labelled with 400 pmol saturation CyDye DIGE fluors (Cy3 or Cy5) and 50 µg of the two pools mix (25 µg from patients' pool and 25 µg from healthy donors' pool) labeled with 400 pmol Cy2. Five micrograms of each sample were reduced with 2 mM Tris (2-carboxyethyl)phosphine (TCEP) for 1 h at 37 °C. Cyanine 3 (Cy3) and cyanine 5 (Cy5) sulfhydryl-reactive dyes (0.8 nmol/µg protein) were added

respectively to REVE2 and standard samples and incubated for 30 min at 37 °C in the dark. The reaction was stopped with the addition of an equal volume of sample buffer containing 7 mol/L urea, 2 mol/L thiourea, 4% CHAPS, 130 mmol/L dithiothreitol (DTT) and, 2% pharmalytes (GE Healthcare).The Cy3-labelled REVE samples were then mixed with Cy5-labelled standard samples and left for 15 min on ice in the dark. Immobilized pH gradient (IPG) strip (240 mm, pH 4–7 linear gradient) was rehydrated with 450 µl of labelled mixed samples in rehydration buffer containing 1% Pharmalytes, 1300 mmol/L DTT, 7 mol/L urea, 2 mol/L thiourea and 4% CHAPS on a Protean IEF cell system (Biorad) for 24 h without applying any current. After rehydration, IEF was performed at 300 volts (V) for 3 h, and then at a gradient to 1000 V for 6 h, at a gradient to 8000 V for 3 h and finally at 8000 V for 3 h with the temperature maintained at 20 °C. After IEF, the IPG strips were incubated in equilibration buffer containing 6 mol/L urea, 0.1 mmol/L Tris-HCl pH 8, 2% w/v sodium dodecyl sulfate (SDS) and 30% v/v glycerol for 10 min at room temperature. The equilibrated IPG strips were transferred for the second dimension (SDS-polyacrylamide gel electrophoresis (PAGE)) onto 12% PAGE gels and seal with low-melting agarose. Electrophoresis was carried out at 20 °C using an Ettan Dalt 6 system (GE Healthcare) at a constant voltage of 70 V overnight followed by 300 V in the dark.

Following electrophoresis, gels were scanned with an Ettan DIGE Imager (GE Healthcare) at excitation/emission wavelengths of 532/580 nm for Cy3 and 633/670 nm for Cy5 to yield images with a pixel size of 100 µm. Gel images were processed with Progenesis SameSpots (v 3.0) from Nonlinear Dynamics Ltd. (Newcastle, UK) as previously described[15]. First, the images were classified by pairs which corresponded to comigration of one standard and one REVE2 sample in the same gel. After choosing the image of reference, the whole 2D-images were automatically aligned in 2 steps (all the standards' images were aligned then each REVE2 sample's image is

aligned with the image of comigrating standard). All gels were compared with the reference gel to normalize spots'values. An average of 429 spots per gel was detected. Each spot was normalized by the ratio between intensities of Cy3-REVE-2 sample and Cy5-standard. We then compared the normalized spots (Cy3-REVE-2/Cy5-standard). Fold values as well as p-values of all spots were calculated by SamesSpots software using one way ANOVA analysis. Differential expression of a protein present in the gels was considered significant when the p value was below 0.05 (one-way ANOVA analysis).

Differentially regulated spots were excised manually from a preparative gel performed with 500 µg of proteins and in-gel digested with trypsin[16]. Identifications were performed by MALDI-TOF with a Voyager DE STR mass spectrometer (PerSeptive Biosystems, Framingham, MA, USA) equipped with a 337.1 nm nitrogen laser and a delayed extraction facility (125 msec). All spectra were acquired in a positive ion reflector mode under 20 kV voltage, 61% grid. The mass spectra were then calibrated before protein identification by peptide mass fingerprinting, conducted by running the MASCOT web searcher (http://www.matrixscience.com, Matrix Science, UK) against the NCBInr 20080718 (6833826 sequences; 2363426297 residues) with the following parameters: Fixed modifications: CyDye-Cy3 (C); Variable modifications: Oxidation (M); Peptide Mass Tolerance: ± 50 ppm; Peptide Charge State: 1+; Max Missed Cleavages: 1 as previously described[15]. Some spots were identified with nano-LC- MS/MS (on an Ultraflex™ TOF/TOF instrument).

RNA extraction and quantitative real time-polymerase chain reaction (qRT-PCR)

RNA was extracted from LV with TRI Reagent (Ambion, Austin, TX, USA) and from NCM with QIAGEN RNeasy Mini Kit (Qiagen), as described by the manufacturers's instructions.

Then, 500 ng of LV RNA and 250 ng of NCM RNA were reverse-transcribed using the miScript II RT kit (Qiagen). qRT-PCR was performed with the miScript SYBR Green PCR kit (Qiagen) on a Mx3005P Q-PCR system (Agilent Technologies), according to the manufacturer's instructions. The sequences of the different primers (Eurogentec) used were: rat ANP (sense: CCGGTACCGAAGATAACAGC and antisense: CTCCAGGAGGGTATTCACCA), rat BNP (sense:CTGGGAAGTCCTAGCCAGTCTCCA and antisense: GCGACTGACTGCGCCGATCCGGTC), rat Clu (sense: GCTCCATAGCCCAGCTTTAC and antisense: ACTTCTCACACTGGCCCTTC), rat GAPDH (sense: GGCATTGCTCTCATTGACAA and antisense: TGTGAGGGAGATGCTCAGTG), and rat HPRT (sense: ATGGGAGGCCATCACATTGT and antisense: ATGTAATCCAGCAGGTCAGCAA-. ΔΔCT method was used for data analysis.

Western blot analysis

Antibodies

The primary antibodies used for western blot analysis were: Clusterin (sc-6419) and GAPDH (sc-365062) antibodies from Santa Cruz Biotechnology; Clusterin (RD182034110) from Biovendor; phospho-Akt (Ser473) (9271), phospho-GSK-3β (Ser9)(9336), phospho-ERK1/2 (Thr202/Tyr204) (4376), Akt (9272), GSK-3β (9315), and ERK1/2 (9102) antibodies from Cell signaling and Sarcomeric-actin (m0874) antibody from Dako. The horseradish peroxidase-labelled secondary antibodies used were: anti-rabbit IgG (NA934V) and anti-mouse IgG (NA931) antibodies from GE healthcare and anti-goat IgG antibody (sc-2020) from Santa Cruz Biotechnology. The dilution of antibodies used for Western blot depended of each sample (see details in the Supplemental Table 1).

Protein extraction

H9c2 and NCM protein extracts were collected by scraping cells into ice-cold RIPA buffer (50 mmol/L Tris pH 7,4, 150 mmol/L NaCl, 1% Igepal (Sigma, CA-630), 50 mmol/L sodium deoxycholate, and 0.1% SDS) containing anti-proteases (Roche, 11836145001/ 1 tablet for 50 mL of buffer), 1 mmol/L sodium orthovanadate (Sigma, S6508) and 1% protein phosphatase inhibitors cocktail 2 and 3 (Sigma, P5726 and P0044). LV extracts were collected by Dounce-Potter homogenisation on ice in RIPA buffer as described above. All extracts were then incubated one h at 4°C and then centrifuged at 11000 rpm, 4°C, for 10 min to remove cellular debris. The samples were kept at -80°C.

Proteins from culture medium (2 mL) were precipitated with 8 mL acetone at -20°C overnight and then centrifuged at 2700 g, 4°C, for 15 min. The pellet was then washed 3 times with 3 mL of cold ethanol and a centrifugation at 2700 g, 4°C, for 10 min is performed after each wash. The protein pellets were then dried and resuspended in 300 µL of RIPA buffer and the samples were stored at -80°C.

Protein concentrations were determined with a Bradford-based method protein assay (Biorad, 500-0006).

Western blot

Proteins (20 µg of NCM, 40 µg of culture media protein, 50 µg of LV protein and 1µl of plasma) were separated on 10% SDS-PAGE and transferred on 0.22 µm nitrocellulose membranes (Trans-Blot® Turbo^{TM} Transfert Pack, Bio-rad). Equal total proteins loads were confirmed by Ponceau red [0.1% Ponceau red, 5% acetic acid (v/v) (Sigma-Aldrich)] staining of the membranes. After blocking with 5% non-fat dry milk in TBS-Tween 0.1% buffer for 1 h at room temperature, the membranes were incubated with primary antibodies at 4°C with gentle shaking overnight as described in supplemental table 1. The membranes were then washed three

times for 10 min with TBS-Tween 0.1% buffer and incubated with the corresponding horseradish peroxidase-labelled secondary antibody for 1h in the blocking solution (see details in the Supplemental table 1). After three washes with TBS-Tween 0.1% buffer, the membranes were incubated with enhanced chemiluminescence (ECL™) western blotting detection reagents (GE Healthcare) according to the manufacturer's instructions.

The Chemidoc® camera (Biorad) was then used for imaging the membranes and densitometric measurements of the bands were analysed with the Image Lab software (Bio-Rad).

Quantification by multiplex immunoassay

B-type natriuretic peptide (BNP) was measured in plasma samples using a Multi Analyte Profiling Kit for simultaneous quantitative detection of rat cardiovascular biomarkers (Rat CVD1 Panel 1, RCVD1-89K Millipore) according to the manufacturer's instructions as previously described [17].

Quantification of clusterin in plasma from REVE-2 and INCA studies

Western blot

Western blot detection of clusterin in plasma of REVE-2 patients was performed with the mouse primary antibody (Hs-3, Biovendor) (1/2000). Briefly, 1 µL of crude plasma proteins was resolved on 12% SDS-PAGE (NuPAGE 10% Bis-Tris gel, Life Technologies), transferred as described above before incubation with horseradish peroxidase-labelled secondary antibody (1/5000) for 1 h in blocking solution.

ELISA

Clusterin in plasma of INCA patients was quantified by ELISA (R&D systems, Minneapolis, MN, USA). The sensitivity was 0.189 ng/mL and the variability between plates estimated

between 3.4-3.7%.by ELISA (R&D systems, Minneapolis, MN, USA). The sensitivity was 0.189 ng/mL and the variability between plates estimated between 3.4-3.7%.

LC-MRM MS with SIS peptides

The peptides had been previously validated for its use in LC-MRM experiments following the CPTAC guidelines for assay development (https://assays.cancer.gov). The tryptic peptide was selected to serve as molecular surrogate for clusterin according to a series of peptide selection rules (*e.g.*, sequence unique, devoid of oxidizable residues; see [18] for detailed criteria) and previous detectability in pooled plasma samples. To help compensate for matrix-induced suppression or variability in LC-MS performance, $^{13}C/^{15}N$-labeled peptide analogues were used as internal standards. The peptides (light and SIS) were synthesized via Fmoc chemistry, purified through RP-HPLC with subsequent assessment by MALDI-TOF-MS, and characterized via amino acid analysis, (AAA), and capillary zone electrophoresis (CZE) with an average CZE-derived purity of 92.4%.

The plasma proteolytic digests were prepared in an automated manner on a Tecan Freedom EVO 150 on a 96-well microplate (Axygen). In the sample preparation, 10 µL of raw plasma was subjected to 9 M urea, 20 mM dithiothreitol, and 0.5 M iodoacetamide (all in Tris buffer at pH 8.0). Denaturation and reduction occurred simultaneously at 37°C for 30 min; with alkylation occurring thereafter in the dark at room temperature for 30 min. Proteolysis was initiated by the addition of TPCK-treated trypsin (35 µL at 1 mg/mL; Worthington) at a 20:1 substrate: enzyme ratio. After overnight incubation at 37°C, proteolysis was quenched with 1% FA. The SIS peptide mixture was then spiked into the digested samples, the standard curve samples, and the QC samples and concentrated by solid phase extraction (SPE) (Oasis HLB, 2 mg sorbent; Waters).

After SPE, the concentrated eluate was frozen, lyophilized to dryness, and rehydrated in 0.1% FA (final concentration: 0.5 µg/µL digest) for LC-MRM/MS.

The standard curve was prepared using a mix of light peptides that was spiked into a human plasma tryptic digest in which the peptides were dimethylated (to shift their masses) from a high concentration of 1000X the Lower limit of quantitation (LLOQ) over 8 dilutions to the lowest point of the curve which was the LLOQ for the assay. The QC samples were prepared from the same light peptide mix and diluted in dimethylated human plasma digest at 4X, 50X, and 500X the LLOQ for each peptide.

Twenty microliters injections of the plasma tryptic digests were separated with a Zorbax Eclipse Plus RP-UHPLC column (2.1 x 150 mm, 1.8 µm particle diameter; Agilent) that was contained within a 1290 Infinity system (Agilent). Peptide separations were achieved at 0.4 mL/min over a 60 min run, via a multi-step LC gradient (2-80% mobile phase B; mobile phase compositions: A was 0.1% FA in H_2O while B was 0.1% FA in ACN). The column was maintained at 40˚C. A post-gradient equilibration of 4 min was used after each sample analysis.

The LC system was interfaced to a triple quadrupole mass spectrometer (Agilent 6490) via a standard-flow ESI source, operated in the positive ion mode. The general MRM acquisition parameters employed were as follows: 3.5 kV capillary voltage, 300 V nozzle voltage, 11 L/min sheath gas flow at a temperature of 250°C, 15 L/min drying gas flow at a temperature of 150°C, 30 psi nebulizer gas pressure, 380 V fragmentor voltage, 5 V cell accelerator potential, and unit mass resolution in the first and third quadrupole mass analysers. The high energy dynode (HED) multiplier was set to -20 kV for improved ion detection efficiency and signal-to-noise ratios. Specific LC-MS acquisition parameters were employed for optimal peptide ionization/fragmentation and scheduled MRM (see supplemental Table 2) for the dynamic MRM

method. Note that the peptide optimizations were empirically optimized previously by direct infusion of the purified SIS peptides. In the quantitative analysis, the targets (with 3 transitions/peptide form) were monitored over 500 ms cycles and 1 min detection windows.

The MRM data was visualized and examined with MassHunter Quantitative Analysis software (version B.07.00; Agilent). This involved peak inspection to ensure accurate selection, integration, and uniformity (in terms of peak shape and retention time) of the SIS and NAT peptide forms. Thereafter, the processed response (*i.e.*, peak area) data was inputted into our in-house developed software tool – Qualis-SIS – for quantitative analysis. After defining a small number of criteria (*i.e.*, $1/x^2$ regression weighting, <20% deviation in a given level's precision and accuracy) for each concentration level of the standard curve, the tool automatically generates and extracts assay-related information from each standard curve. The endogenous protein concentrations in the patient samples are determined through linear regression [19,20].

Statistical analysis

Data summarized as medians with interquartile range (IQR) were analyzed with GraphPad Prism version 6.01 (GraphPad Software, San Diego, CA). Comparisons were made by Kruskal-Wallis test for REVE-2 and INCA, Wilcoxon-Mann-Whitney test and Wilcoxon- signed rank test for animal and in vitro experiments, as appropriate. Correlations were carried out by Spearman correlation test. Results were considered statistically significant if the $p<0.05$.

REFERENCES

1. Fertin M, Hennache B, Hamon M, Ennezat P V., Biausque F, Elkohen M, Nugue O, Tricot O, Lamblin N, Pinet F, Bauters C. Usefulness of Serial Assessment of B-Type Natriuretic Peptide, Troponin I, and C-Reactive Protein to Predict Left Ventricular Remodeling After Acute Myocardial Infarction (from the REVE-2 Study). *Am J Cardiol*. 2010;106:1410–1416.
2. de Groote P, Dagorn J, Soudan B, Lamblin N, McFadden E, Bauters C. B-type natriuretic peptide and peak exercise oxygen consumption provide independent information for risk stratification in patients with stable congestive heart failure. *J Am Coll Cardiol*. 2004;43:1584–1589.
3. De Groote P, Lamblin N, Mouquet F, Plichon D, McFadden E, Van Belle E, Bauters C. Impact of diabetes mellitus on long-term survival in patients with congestive heart failure. *Eur Heart J*. 2004;25:656–662.
4. de Groote P, Fertin M, Goéminne C, Petyt G, Peyrot S, Foucher-Hossein C, Mouquet F, Bauters C, Lamblin N. Right ventricular systolic function for risk stratification in patients with stable left ventricular systolic dysfunction: comparison of radionuclide angiography to echoDoppler parameters. *Eur Heart J*. 2012;33:2672–2679.
5. de Groote P, Fertin M, Duva Pentiah A, Goéminne C, Lamblin N, Bauters C. Long-term functional and clinical follow-up of patients with heart failure with recovered left ventricular ejection fraction after beta-blocker therapy. *Circ Heart Fail*. 2014;7:434–439.
6. Lemesle G, Maury F, Beseme O, Ovart L, Amouyel P, Lamblin N, de Groote P, Bauters C, Pinet F. Multimarker proteomic profiling for the prediction of cardiovascular mortality in patients with chronic heart failure. *PLoS One* . 2015;10:e0119265.

7. Mulder P, Devaux B, Richard V, Henry J, Wimart MC, Thibout E, Macé B, Thuillez C. Early versus delayed angiotensin-converting enzyme inhibition in experimental chronic heart failure. Effects on survival, hemodynamics, and cardiovascular remodeling. *Circulation*. 1997;95:1314–1319.

8. Pfeffer M, Pfeffer J, Steinberg C, Finn P. Survival after an experimental myocardial infarction: beneficial effects of long-term therapy with captopril. *Circulation*. 1985;72:406–412.

9. Dubois E, Richard V, Mulder P, Lamblin N, Drobecq H, Henry J-P, Amouyel P, Thuillez C, Bauters C, Pinet F. Decreased serine207 phosphorylation of troponin T as a biomarker for left ventricular remodelling after myocardial infarction. *Eur Heart J* . 2011;32:115–123.

10. Mulder P, Barbier S, Chagraoui A, Richard V, Henry JP, Lallemand F, Renet S, Lerebours G, Mahlberg-Gaudin F, Thuillez C. Long-term heart rate reduction induced by the selective I(f) current inhibitor ivabradine improves left ventricular function and intrinsic myocardial structure in congestive heart failure. *Circulation*. 2004;109:1674–1679.

11. Dubois-Deruy E, Belliard A, Mulder P, Bouvet M, Smet-Nocca C, Janel S, Lafont F, Beseme O, Amouyel P, Richard V, Pinet F. Interplay between troponin T phosphorylation and O-N-acetylglucosaminylation in ischaemic heart failure. *Cardiovasc Res*. 2015;107:56–65.

12. Thulasiraman V, Lin S, Gheorghiu L, Lathrop J, Lomas L, D H, Boschetti E. Reduction of the concentration difference of proteins in biological liquids using a library of combinatorial ligands. *Electrophoresis*. 2005;26:3561–3571.

13. Guerrier L, Thulasiraman V, Castagna A, F F, S L, Lomas L, Righetti PG, Boschetti E.

Reducing protein concentration range of biological samples using solid-phase ligand libraries. *J Chromatogr B Anal Technol Biomed Life Sci*. 2006;833:33–40.

14. Fertin M, Beseme O, Duban S, Amouyel P, Bauters C, Pinet F. Deep plasma proteomic analysis of patients with left ventricular remodeling after a first myocardial infarction. *Proteomics Clin Appl*. 2010;4:654–673.
15. Acosta-Martin AE, Chwastyniak M, Beseme O, Drobecq H, Amouyel P, Pinet F. Impact of incomplete DNase I treatment on human macrophage proteome analysis. *Proteomics Clin Appl*. 2009;3:1236–46.
16. Shevchenko A, Jensen ON, Podtelejnikov AV, Sagliocco F, Wilm M, Vorm O, Mortensen P, Shevchenko A, Boucherie H, Mann M. Linking genome and proteome by mass spectrometry: large-scale identification of yeast proteins from two dimensional gels. *Proc Natl Acad Sci U S A*. 1996;93:14440–14445.
17. Dubois-Deruy E, Belliard A, Mulder P, Chwastyniak M, Beseme O, Henry J-P, Thuillez C, Amouyel P, Richard V, Pinet F. Circulating plasma serine208-phosphorylated troponin T levels are indicator of cardiac dysfunction. *J Cell Mol Med*. 2013;17:1335–44.
18. Kuzyk MA, Parker CE, Domanski D, Borchers CH. Development of MRM-based assays for the absolute quantitation of plasma proteins. *Methods Mol Biol*. 2013;1023:53–82.
19. Percy AJ, Chambers AG, Yang J, Hardie DB, Borchers CH. Advances in multiplexed MRM-based protein biomarker quantitation toward clinical utility. *Biochim Biophys Acta*. 2014;1844:917–926.
20. Mohammed Y, Percy AJ, Chambers AG, Borchers CH. Qualis-SIS: automated standard curve generation and quality assessment for multiplexed targeted quantitative proteomic experiments with labeled standards. *J Proteome Res*. 2015;14:1137–1146.

Supplemental Table 1: List and dilution of antibodies used for western blot analysis

Primary antibodies	Reference	Incubation buffer	Sample :Dilution	Secondary antibodies	Dilution
Clusterin	sc-6419, Santa Cruz	TBST-0.1% + 5% Milk	H9c2 : 1/500	Anti-goat antibody (sc-2020, Santa Cruz)	1/10000
			NCM Media : 1/2000		1/10000
			NCM Lysate : 1/500		1/10000
			Rat LV : 1/1000		1/5000
			Human cardiac biopsies : 1/20000		1/40000
Clusterin	RD182034110, Biovendor		Human plasma : 1/2000	Anti-mouse antibody (NA931, GE Healthcare)	1/5000
pAkt (Ser473)	9271, Cell Signalling	TBST-0.1% + 5% BSA	1/500	Anti-rabbit antibody (NA934V, GE	1/5000
Akt	9272, Cell Signalling		1/2000		1/5000

pERK1/2 (Thr202/Tyr204)	4376, Cell Signalling		1/500	Healthcare)	1/5000
ERK1/2	9102, Cell Signalling		1/5000		1/5000
pGSK (Ser9)	9336, Cell Signalling		1/3000		1/10000
GSK	9315, Cell Signalling		1/5000		1/10000
S-Actin	mo74, Dako	TBST-0.1% + 5% Milk	1/5000	Anti-mouse antibody (NA931, GE Healthcare)	1/10000
GAPDH	sc-36506, Santa Cruz		Rat LV : 1/5000		1/10000
			Human cardiac biopsies : 1/10000		1/20000

TBST : Tris Buffered Saline Tween

Supplemental Table 2. Specific acquisition parameters for the target peptides for clusterin (P10909) measured by bottom-up LC-MRM/MS.

Compound Name	Compound Group	Ion	NAT		SIS		RT (min)	CE (V)
			Q1 *m/z*	Q3 *m/z*	Q1 *m/z*	Q3 *m/z*		
Clusterin	ELDESLQVAER	y3.heavy	644.83	602.33	649.83	385.21	21	12.65
Clusterin	ELDESLQVAER	Y5.heavy	644.83	1046.52	649.83	612.33	21	12.65
Clusterin	ELDESLQVAER	Y9.heavy	644.83	375.21	649.83	1056.52	25	12.65
Clusterin	EPQDTYHYLPFSLPHR	y12+++.heavy	500.75	549.28	503.25	514.27	9	21.76
Clusterin	EPQDTYHYLPFSLPHR	y13+++.heavy	500.75	409.23	503.25	552.61	9	21.76
Clusterin	EPQDTYHYLPFSLPHR	y3.heavy	500.75	510.93	503.25	419.24	17	21.76
Clusterin	TLLSNLEEAK	b2.heavy	559.31	790.39	563.32	215.14	17	19.65
Clusterin	TLLSNLEEAK	y7.heavy	559.31	903.48	563.32	798.41	17	19.65
Clusterin	TLLSNLEEAK	y8.heavy	559.31	215.14	563.32	911.49	17	19.65

The fragmentation and cell acceleration voltages were 380 and 5 V, respectively, for all transitions.

Supplemental Table 3 : Identification by MALDI-MS of the 2D spots selected in Figure 1.

Spot number*	Accession number	Protein name	M*r* (Da) Theo	Exp	p*I* Theo	Exp	MASCOT score	Number of matched peptides/total peptides	Sequence coverage (%)	Peptides M*r* (Exp)
842 853 873	P10909	Clusterin	59184	40000	5.89	4.75	65	6 / 24	12	1887.8214 1903.8205 1392.6909 1074.5735 949.4149 1872.9244

*Number corresponds to the spots visualized in Figure 1B

Supplemental Table 4: Histomorphometric and echocardiographic parameters of rats at 7 days and 2 months post-MI.

	7 days post-MI		2 months post-MI	
	Sham	**MI**	**Sham**	**MI**
Number	8	8	11	11
BW (g)	338 [311-340]	313 [294-327]	450 [437-466]	447 [415-472]
HW (g)	0.97 [0.90-1.02]	1,04 [1.02-1.1]*	1.35 [1.29-1.43]	1.67 [1.57-1.76]***
LVW (g)	0.73 [0.65-0.75]	0.73 [0.67-0.76]	1.01 [0.97-1.04]	1.25 [1.2-1.3]**
(HW/ BW) *10^3	2.9 [2.8-3.2]	3.3 [3.1-3.7]*	3 [2.8-3.2]	3.6 [3.3-4.3]**
(LVW/BW) *10^3	2.2 [2-2.3]	2.3± [2.3-2.4]*	2.2 [2.1-2.4]	2.7 [2.4-3.3]**
LVEDD (mm)			6.6 [6.1-7.1]	10.3 [9.3-11.5]***
LVESD (mm)			3.3 [2.9-4.2]	8.7 [7.4-10]***
FS (%)			49 [40-52]	14 [11-20]***
HR (bpm)			439 [396-467]	420 [377-463]
SV (ml)			0.38 [0.38-0.47]	0.34 [0.25-0.37]
CO (ml/min)			169 [132-195]	137 [104-166]

MI: myocardial infarction, BW: body weight, HW: heart weight, LVW: left ventricle weight, LVEDD : left ventricle end-diastolic diameter, LVESD : left ventricle end-systolic diameter, FS : fractional shortening, HR : Heart rate, SV: stroke volume, CO : cardiac output. Data are expressed as median with 25th and 75th percentiles and statistical significance was determined by Wilcoxon- Mann Whitney. *P<0.05, **P<0.01, ***P<0.001 vs sham rats of the same group.

FIGURE LEGENDS

Supp. Figure 1: Detailed 2D-spots and mass spectra corresponding to clusterin spots in 2D gels. Enlarged corresponding 2D-spot in plasma sample analyzed for each conditions, high LVR (n=5) and no LVR (n=5). The corresponding spot quantified by Progenesis SameSpots is circled for each sample.

Supp. Figure 2: Clusterin analysis in plasma of REVE-2 patients at 1 year post-MI. **A:** Representative 2D-DIGE gel and bioinformatic analysis of spots surrounded corresponding to clusterin in pooled plasma of patients with the lowest and highest percent of LVR at 1 year post-MI. The spot 1031 corresponded to spots 842 and 853 observed in 3 months post-MI. **B**: Quantification by ELISA of clusterin in plasma of 45 REVE-2 patients at 1 year post-MI. Patients were divided by EDV calculated at 1 year with low EDV (<56 mm^2, n=22) and high EDV (56 mm^2, n=23). Data are expressed µg/mL and presented as box and whisker plots showing median (line) and min to max (whisker). Statistical significance was determined by Wilcoxon-Mann Whitney test.*P<0.05 vs low EDV.

Supp. Figure 3: Quantification of cardiac hypertrophic markers and clusterin in sham- and MI-rats. **A**: Quantification by qPCR, of ANP (left panel) and BNP (right panel) expression in the LV of sham- and MI-rats at 7 days (n=8/group) and 2 months (n=9/group) post-MI. HPRT was used to normalize ANP and BNP expression and data are expressed in arbitary units (A.U.). **B**: Quantification by multiplex immunoassay of BNP levels in the plasma of sham- and MI-rats at 7 days (n=8/group) and 2 months (n=11/group). Data are expressed in pg/ml. Data in (A) and (B) are presented as box and whisker plots showing median (line) and min to max (whisker) and statistical significance was determined by Wilcoxon- Mann Whitney test. *P<0.05, **P<0.01,

***P<0.001 *vs* sham rats. **C:** Quantification by western blot of levels of clusterin precursor (p-CLU) and mature (m-CLU) forms in LV of sham- and MI-rats at 7 days (n=8/group) and 2 months (n=11/group) post-MI. GAPDH was used to normalize CLU levels. Data are expressed in fold change in CLU levels relative to Sham p-CLU at 7 days (left panel) and 2 months (right panel) and presented as box and whisker plots showing median (line) and min to max (whisker). Statistical significance was determined by Wilcoxon-Mann Whitney test. ** P<0.01, *** P<0.001 *vs* p-CLU.

Supp. Figure 4: Effect of adrenergic and angiotensin stimulation on clusterin secretion and signaling pathways in H9c2 cells. **A:** Representative western blot (left panel) and quantification (right panel) of secreted clusterin levels (s-CLU) in culture media of H9c2 cells untreated (cont.) or treated by phenylephrine (PE, 20 µmol/L), isoproterenol (ISO, 10 µmol/L) or angiotensin II (AII, 2 µmol/L) for 48 (n=3/ group) and 72h (n=4/group). Red ponceau (RP) was used to normalize s-CLU levels. Graphs show individual and median fold change in CLU levels ± IQR (25%-75%) relative to control cells. **B**: Representative western blots (left panels) and quantification (right panels) of active form (phosphorylated/total ratio) of Akt, GSK-3β and ERK1/2 in 72h ISO-treated cells compared to control cells (n=7 to 9/group). Data are expressed in fold change in active proteins levels relative to control cells and presented as box and whisker plots showing median (line) and min to max (whisker). Statistical significance was determined by Wilcoxon-Mann Whitney test. *P<0.05, **P<0.01 *vs* control cells.

A

2D-DIGE gel

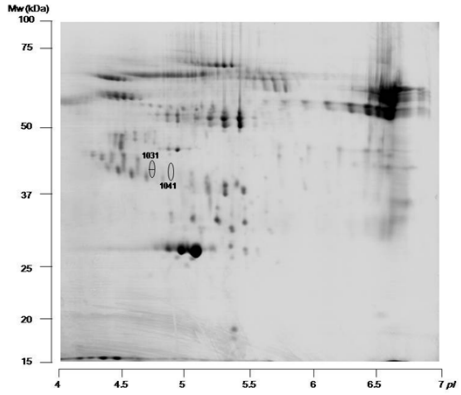

Differential proteomic analysis

Spot	Fold	*P*-value
1031	1.6	0.030
1041	1.7	0.034

Clusterin (P10909)

B

ELISA analysis

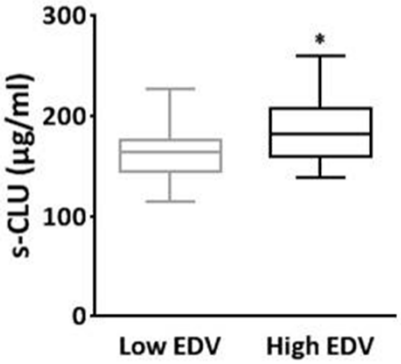

Supplemental Figure 2

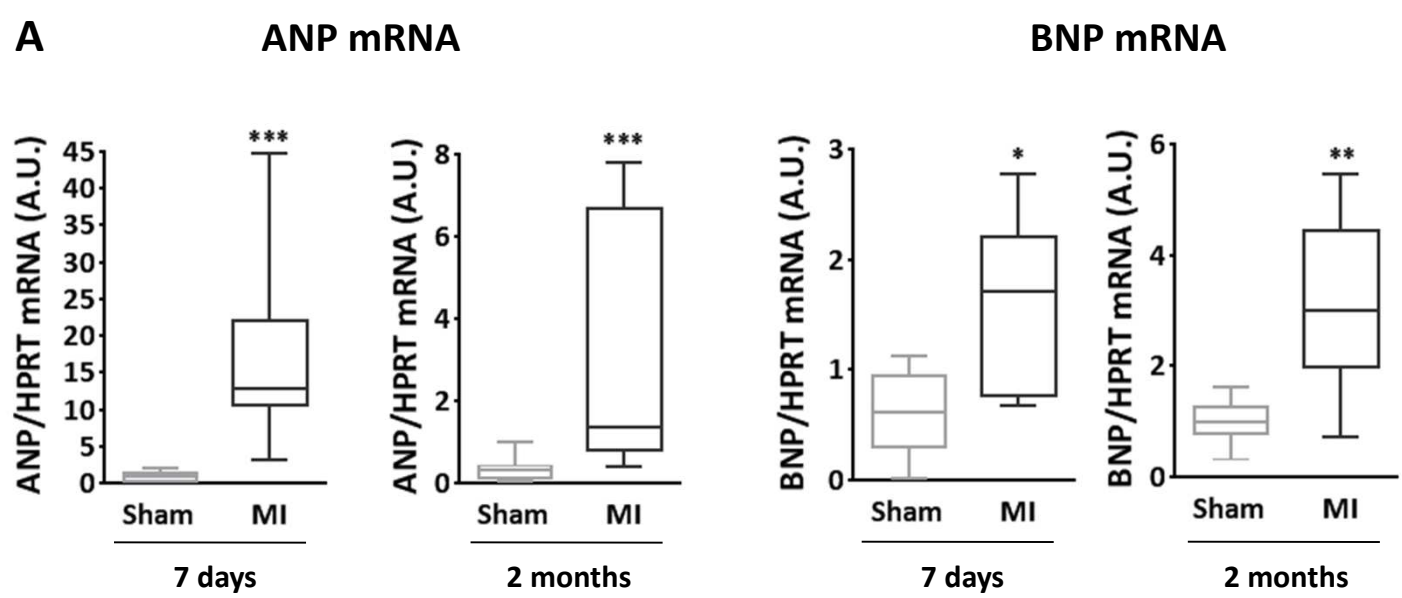

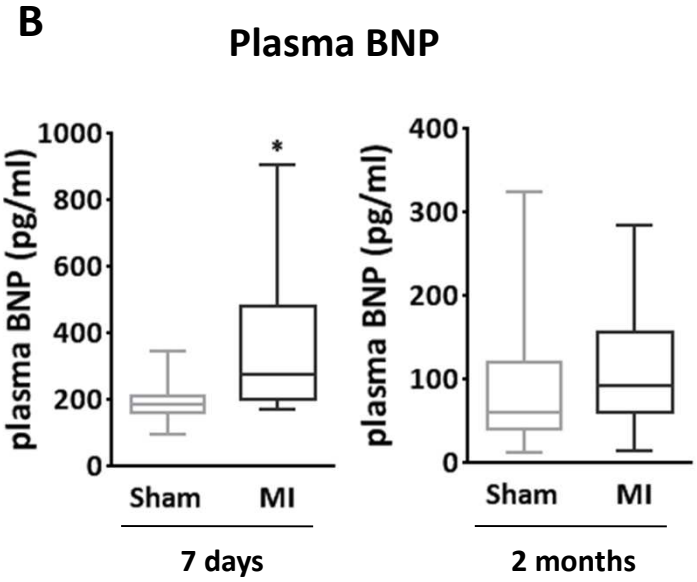

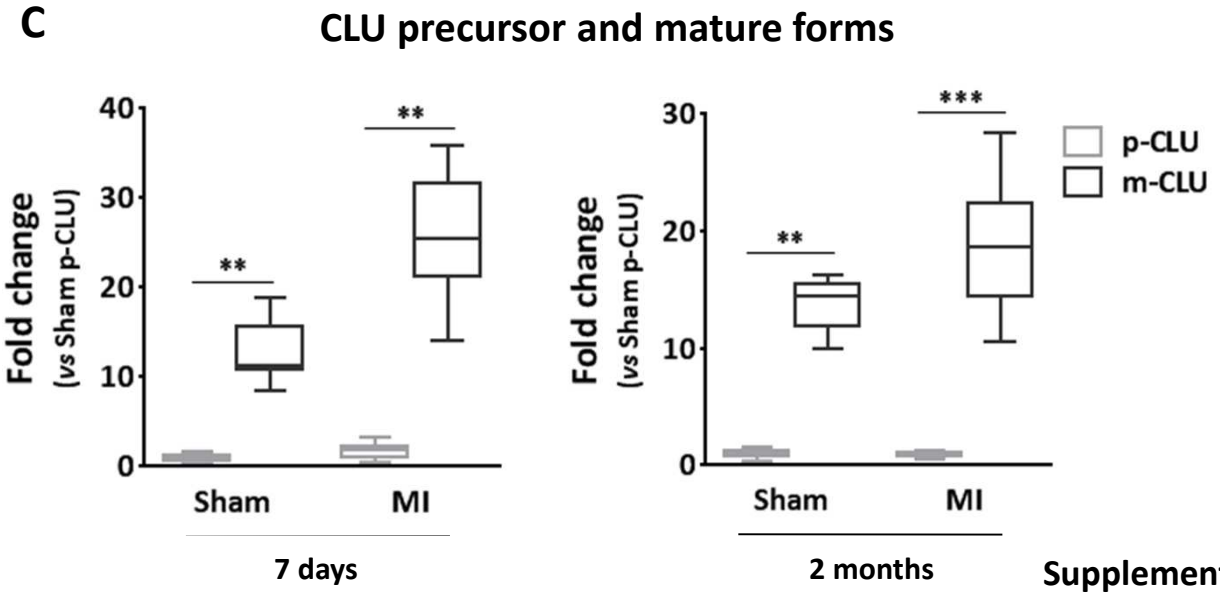

Supplemental Figure 3

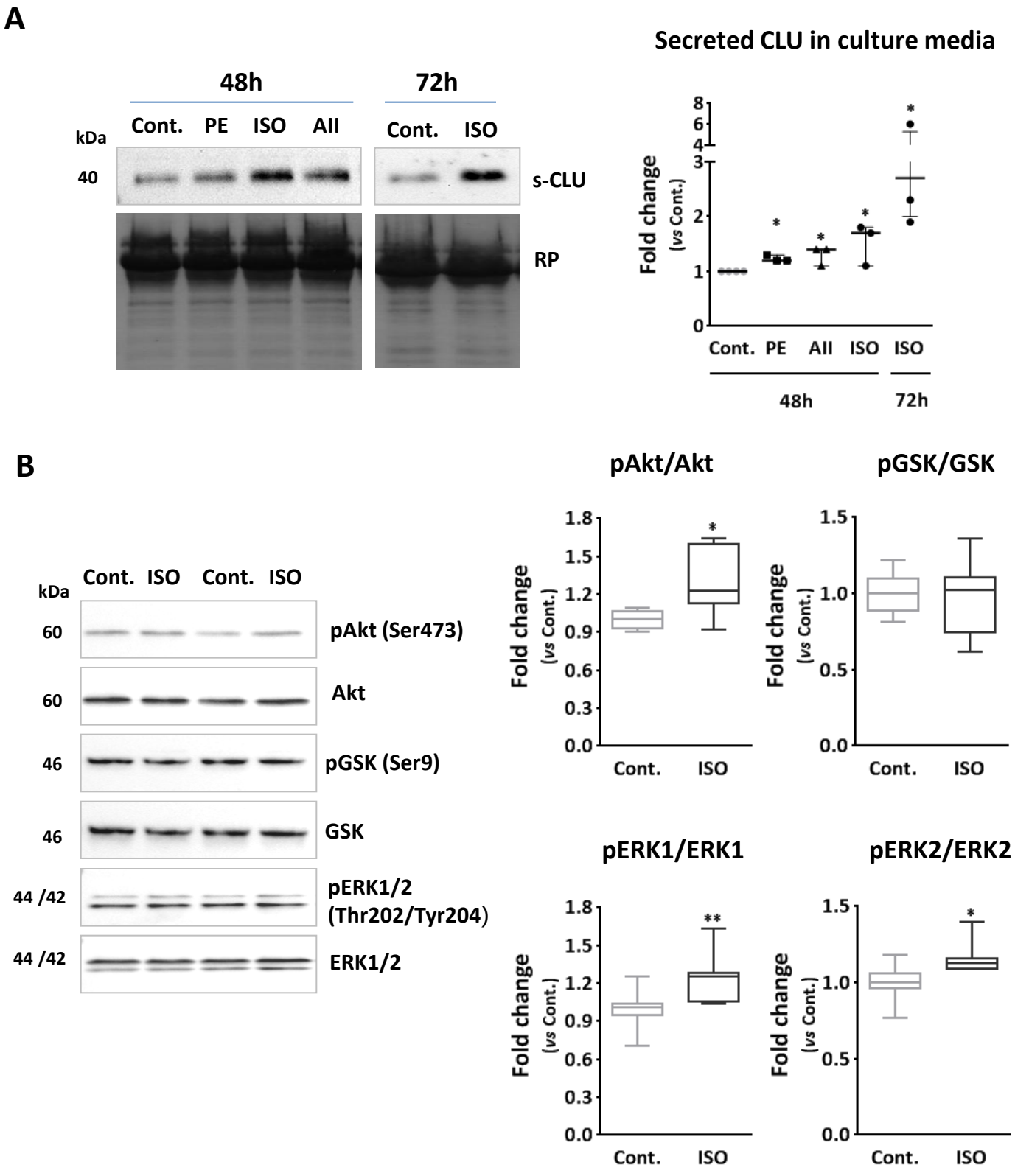

Supplemental Figure 4

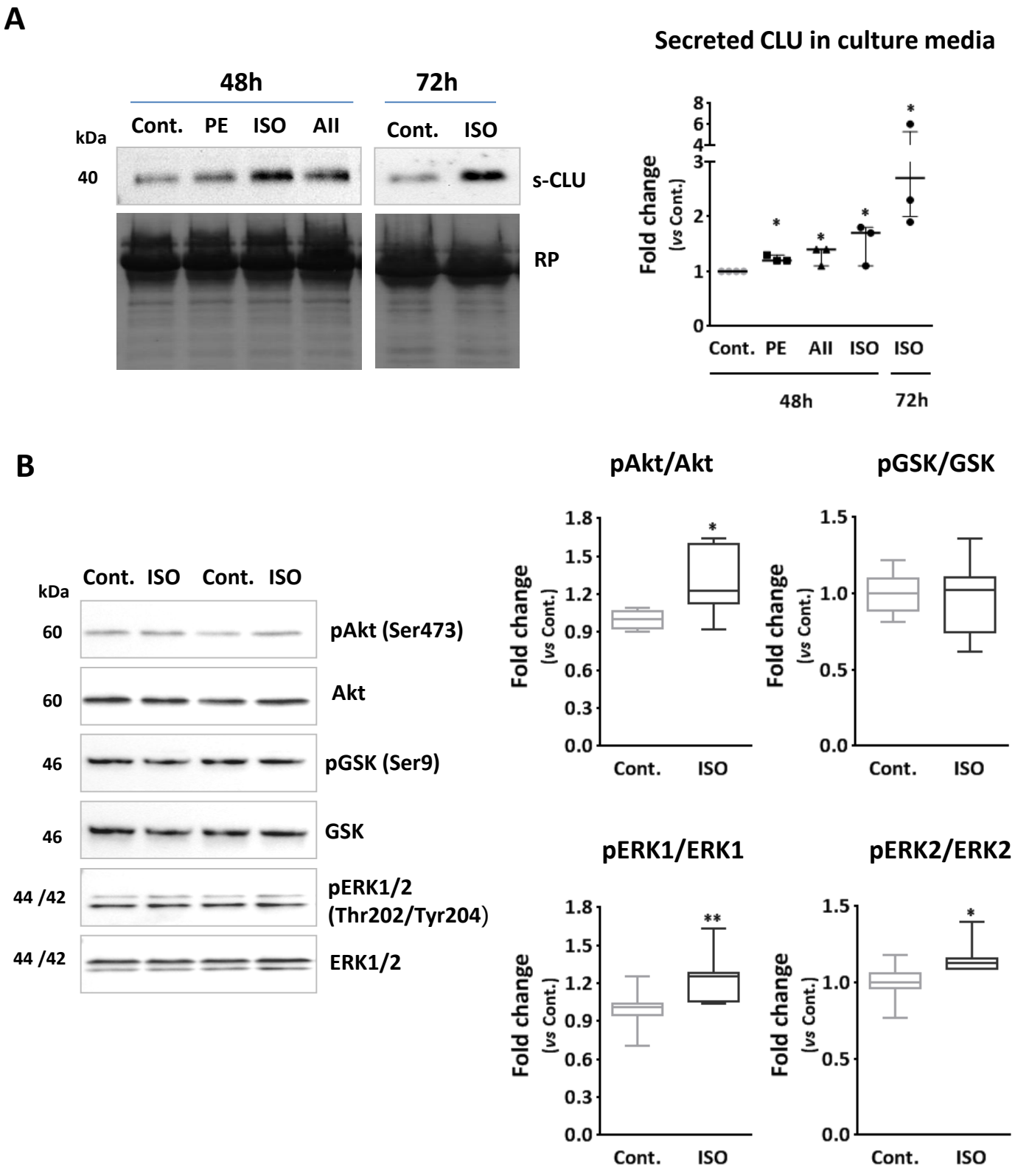

Supplemental Figure 4

A

2D-DIGE gel

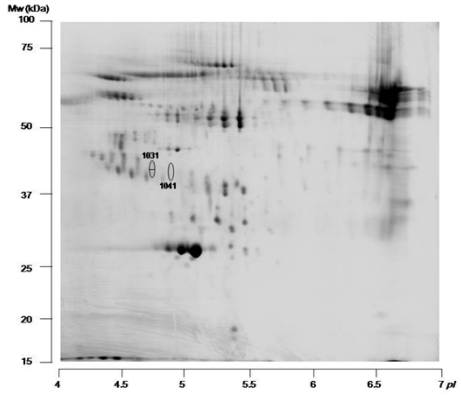

Differential proteomic analysis

Spot	Fold	*P*-value
1031	1.6	0.030
1041	1.7	0.034

Clusterin (P10909)

B

ELISA analysis

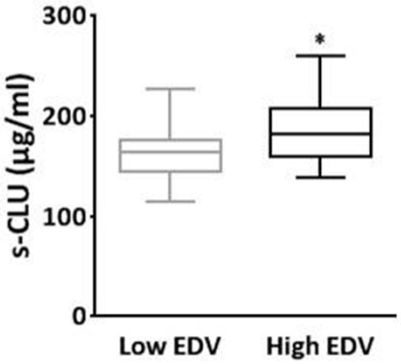

Supplemental Figure 2

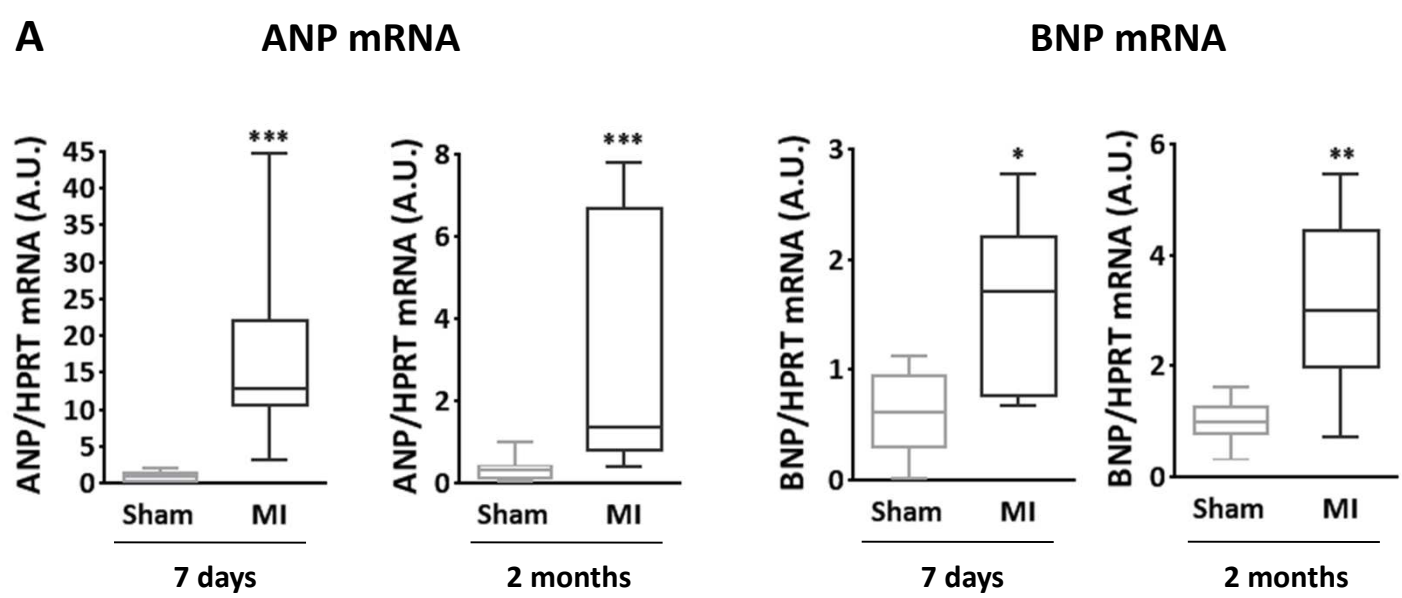

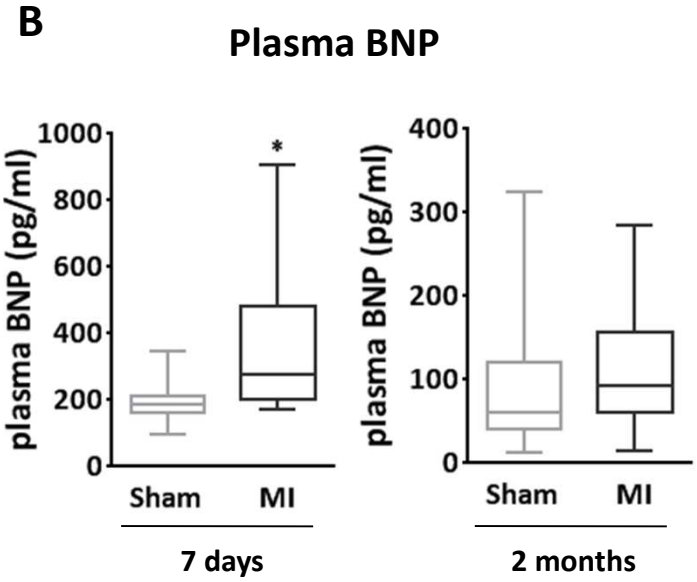

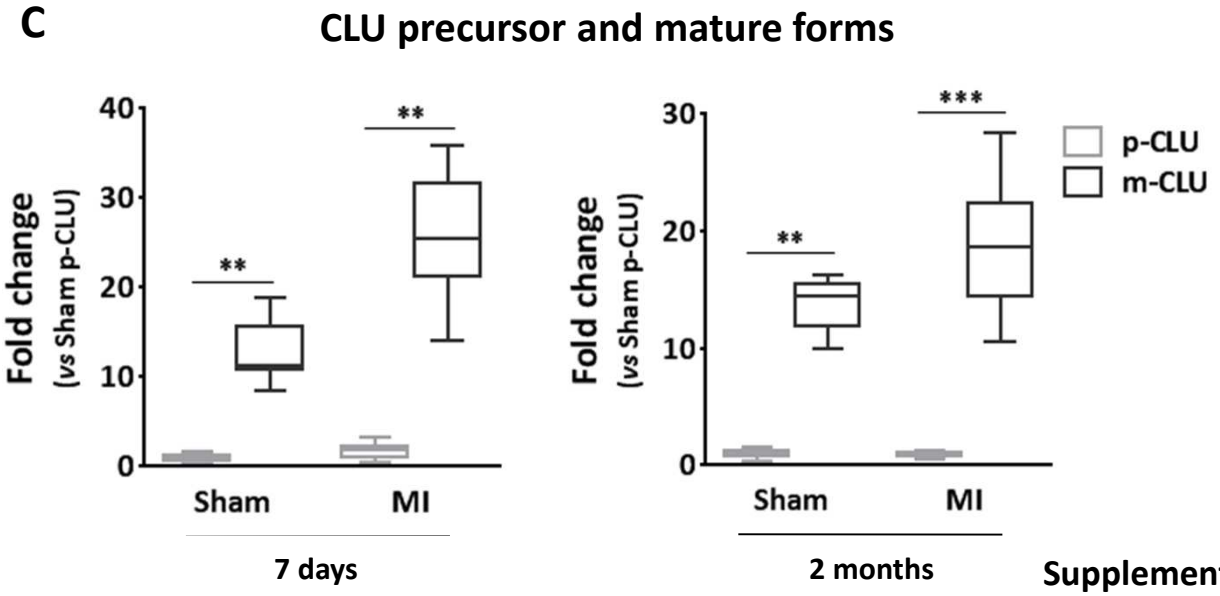

Supplemental Figure 3

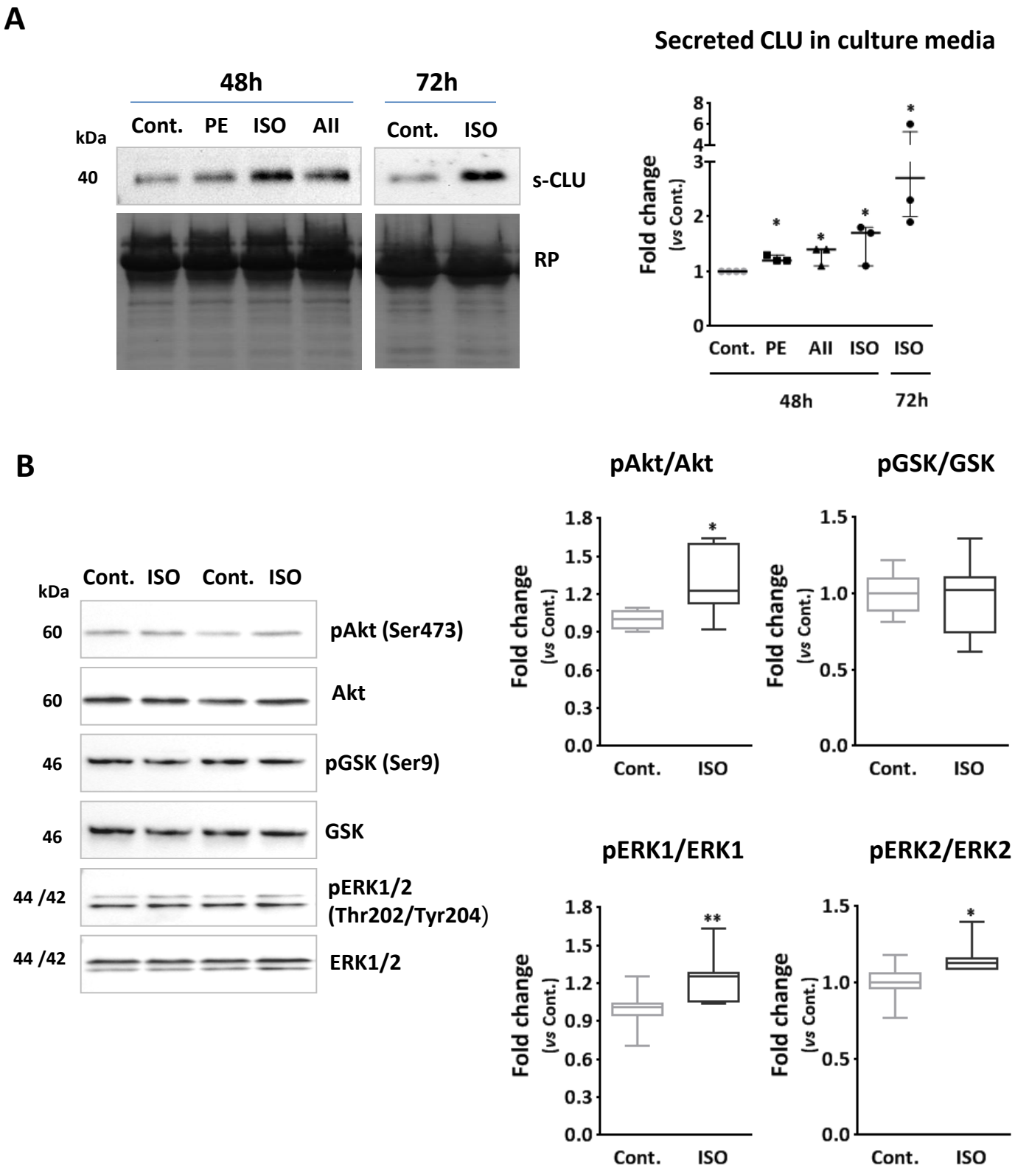

Supplemental Figure 4